

The meson production reactions: the analysis methods and recent results

Andrey Sarantsev

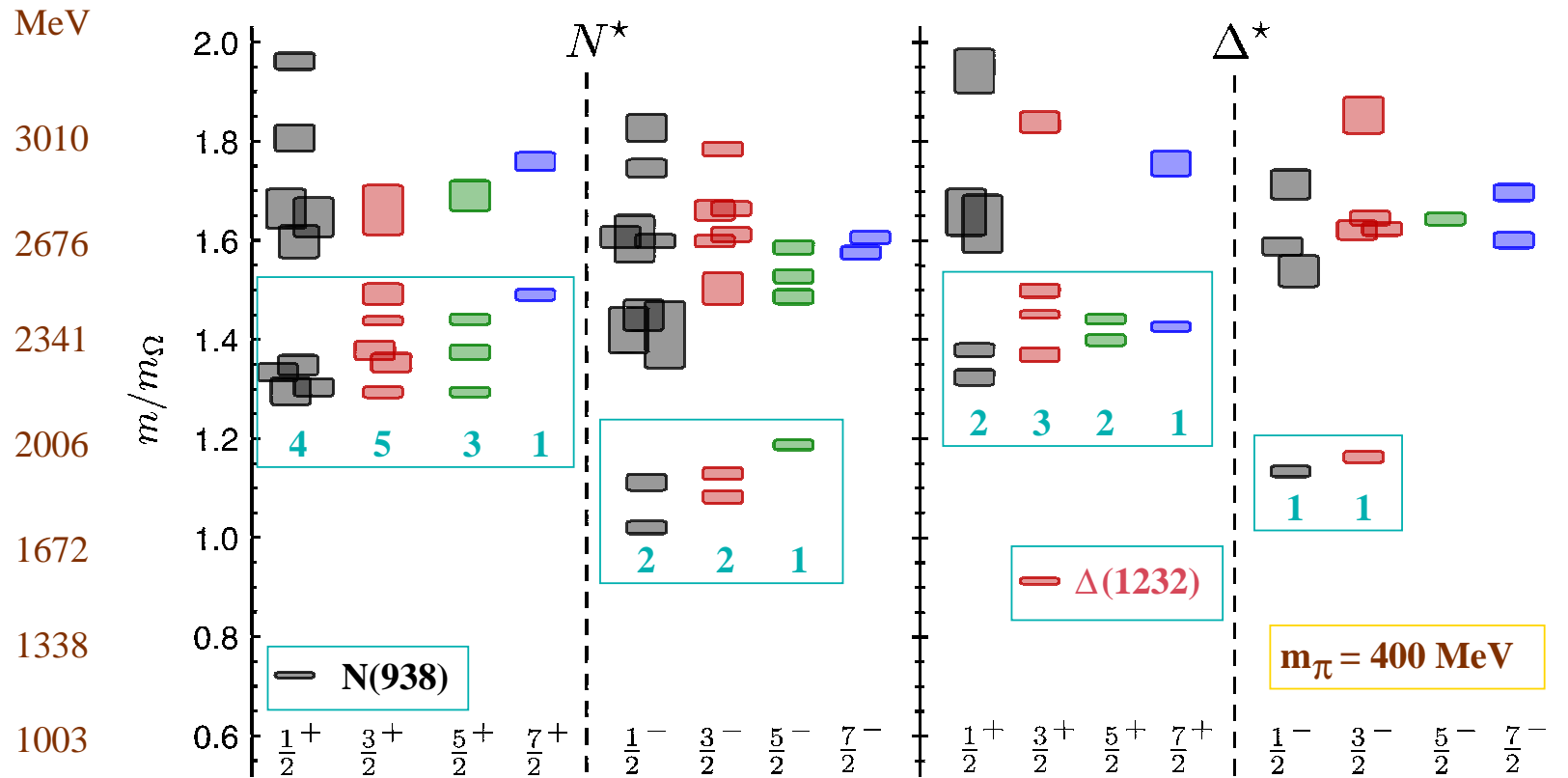


Petersburg
Nuclear
Physics
Institute

HISKP Uni-Bonn (Germany)
PNPI (Russia)

15th International Workshop on Meson Physics KRAKÓW, POLAND, 7th - 12th June 2018

0.0.1 Baryons on the lattice



R.Edwards et al.,
arXiv:1104.5152 [hep-ph]

a Lattice and quark models predict more states than observed (missing resonances)

b Lattice and quark models predict even-odd staggering (exp: parity doublets)

c $3/2^+$: 5 states expected, $N(1720)3/2^+$, $N(1900)3/2^+$, tentative $N(1960)3/2^+$,
 $N(2200)3/2^+$

Baryon sector: the partial wave analysis groups

- **SAID (GWU,USA):** Analysis of elastic πN data in energy independent method and then in the K-matrix approach. Fit of the $\gamma n \rightarrow \pi N, \eta N$ data as a sum of BW amplitudes and now also in the framework of K-matrix/P-vector approach. Recently: analysis of the final states with 2 pions and $\bar{K} N$ collision reactions.
- **MAID (Mainz):** Energy dependent analysis of photoproduction data on γN to $\pi N, \eta p, \eta' p, K \Lambda, K \Sigma$. Parameterization of partial waves as a sum of Breit-Wigner amplitudes with unitarisation procedure. Development of the approach which takes into account crossing symmetry and dispersion corrections.
- **Bonn-Gatchina:** Energy dependent analysis of pion induced (inelastic) and almost all photoproduction data. K-matrix/P-vector and now N/D-dispersion approach. Minimization: χ^2 for 2 body final state and maximum likelihood for multi-body final states. Recently, the analysis of the $\bar{K} N$ collision reactions.
- **Juelich group:** Energy dependent covariant approach. Pion induced data (elastic and inelastic), $\gamma p \rightarrow \pi N, \eta N, K \Lambda, K \Sigma$. Unitarity, analyticity and chiral constraints. Solution of the Bethe-Salpeter equation.

- **ANL-OSAKA Energy dependent covariant approach. Pion induced data (elastic and inelastic), $\gamma p \rightarrow \pi N, \eta N$ (all data) and $\gamma p \rightarrow K\Lambda, K\Sigma$. Unitarity and analyticity constraints. Solution of the Bethe-Salpeter equation. Analysis of the KN collision data with one meson in the final state.**
- **M. Manley (Kent Uni) Energy dependent covariant approach. Pion induced data (elastic and inelastic including 2pion production), $\gamma p \rightarrow \pi N$ (all data) and $\gamma p \rightarrow K\Lambda, K\Sigma$. Unitarity and analyticity constraints.**

Bonn-Gatchina partial wave analysis group:

A. Anisovich, E. Klempt, V. Nikonov, A. Sarantsev, U. Thoma.

<http://pwa.hiskp.uni-bonn.de/>



Bonn-Gatchina Partial Wave Analysis



Address: Nussallee 14-16, D-53115 Bonn Fax: (+49) 228 / 73-2505

[Data Base](#)

[Meson Spectroscopy](#)

[Baryon Spectroscopy](#)

[NN-interaction](#)

[Formalism](#)

Analysis of Other Groups

- [SAID](#)
- [MAID](#)
- [Giessen Uni](#)

BG PWA

- [Publications](#)
- [Talks](#)
- [Contacts](#)

Useful Links

- [SPIRES](#)
- [PDG Homepage](#)
- [Durham Data Base](#)
- [Bonn Homepage](#)

[CB-ELSA Homepage](#)

Responsible: Dr. V. Nikonov, E-mail: nikonov@hiskp.uni-bonn.de
Last changes: January 26th, 2010.

Energy dependent approach

In many cases an unambiguous partial wave decomposition at fixed energies is impossible. Then the energy and angular parts should be analyzed together:

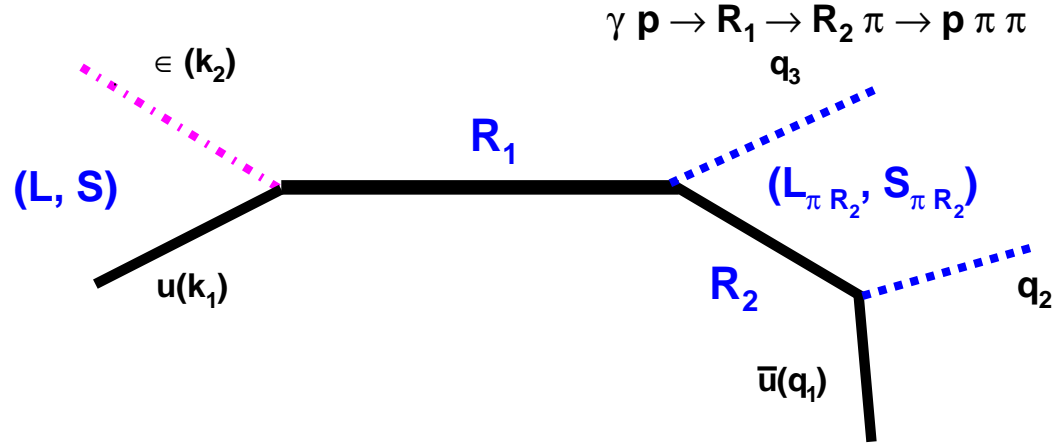
$$A(s, t) = \sum_{\beta\beta'n} A_n^{\beta\beta'}(s) Q_{\mu_1 \dots \mu_n}^{(\beta)+} F_{\nu_1 \dots \nu_n}^{\mu_1 \dots \mu_n} Q_{\nu_1 \dots \nu_n}^{(\beta')}$$

1. A. V. Anisovich, V. V. Anisovich, V. N. Markov, M. A. Matveev and A. V. Sarantsev, J. Phys. G 28, 15 (2002)
2. A. Anisovich, E. Klempt, A. Sarantsev and U. Thoma, Eur. Phys. J. A 24, 111 (2005)
3. A. V. Anisovich and A. V. Sarantsev, Eur. Phys. J. A 30, 427 (2006)
4. A. V. Anisovich, V. V. Anisovich, E. Klempt, V. A. Nikonov and A. V. Sarantsev, Eur. Phys. J. A 34, 129 (2007).

1. Correlations between angular part and energy part are under control.
2. Unitarity and analyticity can be introduced from the beginning.
3. Parameters can be fixed from a combined fit of many reactions.

1. C. Zemach, Phys. Rev. 140, B97 (1965); 140, B109 (1965).
2. S.U.Chung, Phys. Rev. D 57, 431 (1998).
3. B. S. Zou and D. V. Bugg, Eur. Phys. J. A 16, 537 (2003)

Resonance amplitudes for meson photoproduction



General form of the angular dependent part of the amplitude:

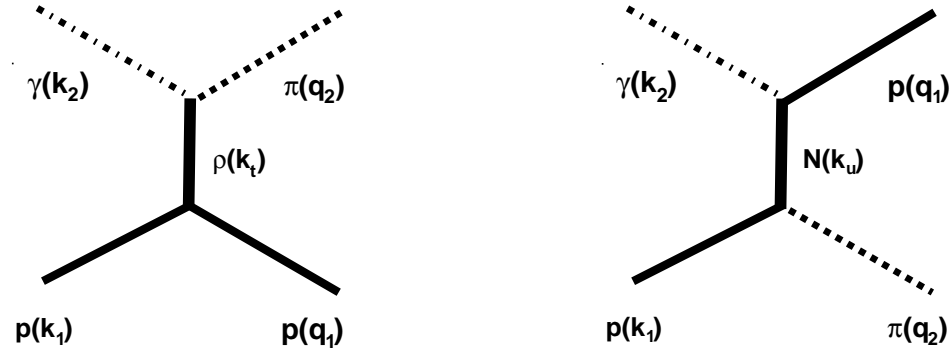
$$\bar{u}(q_1) \tilde{N}_{\alpha_1 \dots \alpha_n} (R_2 \rightarrow \mu N) F_{\beta_1 \dots \beta_n}^{\alpha_1 \dots \alpha_n} (q_1 + q_2) \tilde{N}_{\gamma_1 \dots \gamma_m}^{(j) \beta_1 \dots \beta_n} (R_1 \rightarrow \mu R_2)$$

$$F_{\xi_1 \dots \xi_m}^{\gamma_1 \dots \gamma_m} (P) V_{\xi_1 \dots \xi_m}^{(i) \mu} (R_1 \rightarrow \gamma N) u(k_1) \varepsilon_\mu$$

$$F_{\nu_1 \dots \nu_L}^{\mu_1 \dots \mu_L} (p) = (m + \hat{p}) O_{\alpha_1 \dots \alpha_L}^{\mu_1 \dots \mu_L} \frac{L+1}{2L+1} \left(g_{\alpha_1 \beta_1}^\perp - \frac{L}{L+1} \sigma_{\alpha_1 \beta_1} \right) \prod_{i=2}^L g_{\alpha_i \beta_i} O_{\nu_1 \dots \nu_L}^{\beta_1 \dots \beta_L}$$

$$\sigma_{\alpha_i \alpha_j} = \frac{1}{2} (\gamma_{\alpha_i} \gamma_{\alpha_j} - \gamma_{\alpha_j} \gamma_{\alpha_i})$$

Reggeized exchanges:



The amplitude for t-channel exchange:

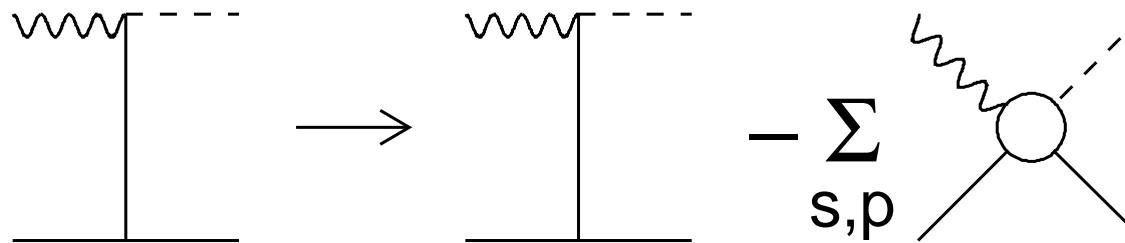
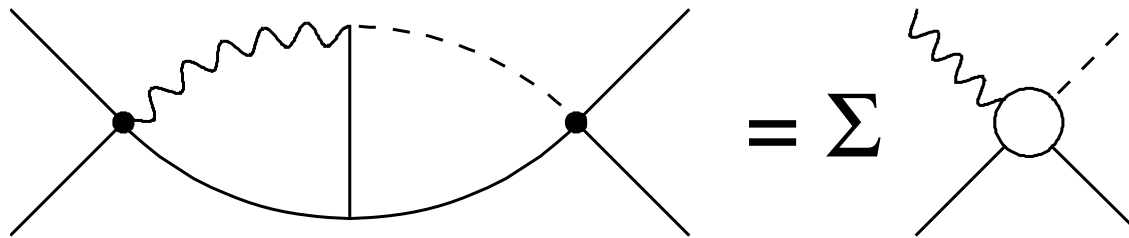
$$A = g_1(t)g_2(t)R(\xi, \nu, t) = g_1(t)g_2(t) \frac{1 + \xi \exp(-i\pi\alpha(t))}{\sin(\pi\alpha(t))} \left(\frac{\nu}{\nu_0} \right)^{\alpha(t)} \quad \nu = \frac{1}{2}(s - u).$$

Here $\alpha(t)$ is the reggion trajectory, and ξ is its signature:

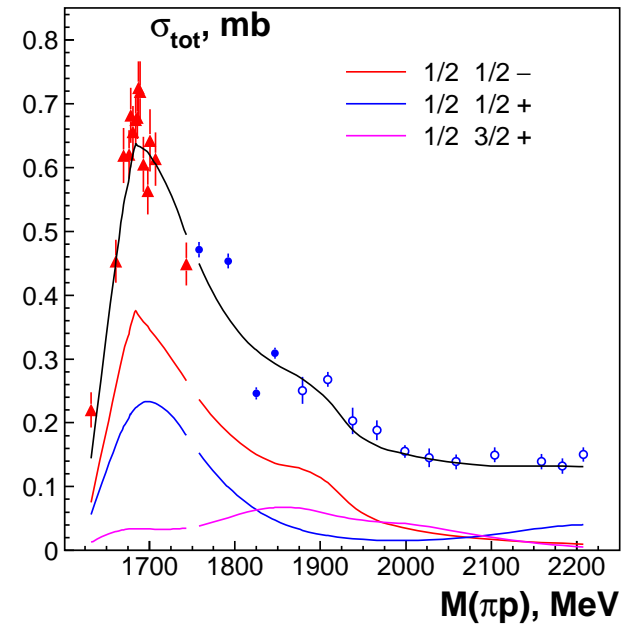
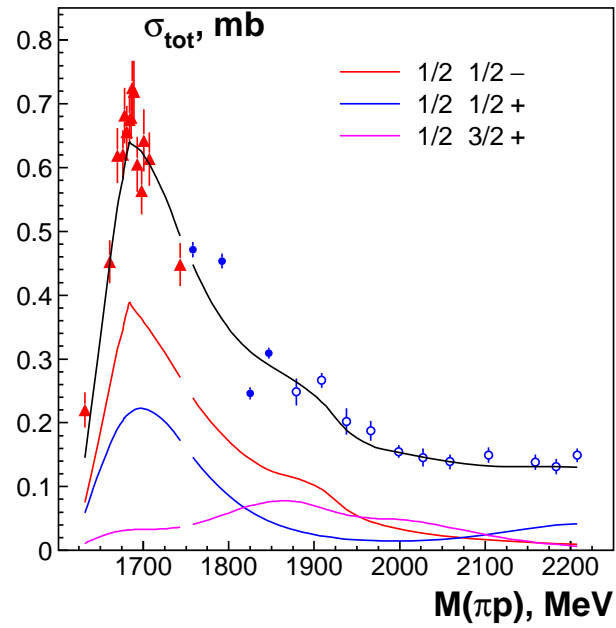
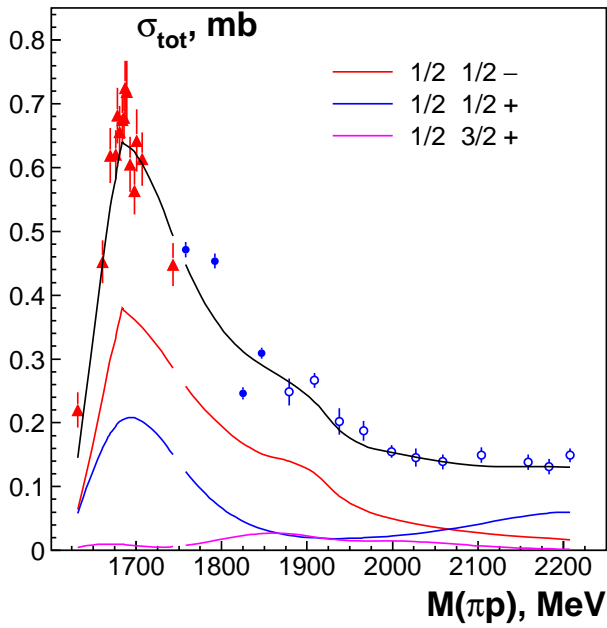
$$R(+, \nu, t) = \frac{e^{-i\frac{\pi}{2}\alpha(t)}}{\sin(\frac{\pi}{2}\alpha(t))\Gamma\left(\frac{\alpha(t)}{2}\right)} \left(\frac{\nu}{\nu_0} \right)^{\alpha(t)},$$

$$R(-, \nu, t) = \frac{ie^{-i\frac{\pi}{2}\alpha(t)}}{\cos(\frac{\pi}{2}\alpha(t))\Gamma\left(\frac{\alpha(t)}{2} + \frac{1}{2}\right)} \left(\frac{\nu}{\nu_0} \right)^{\alpha(t)}.$$

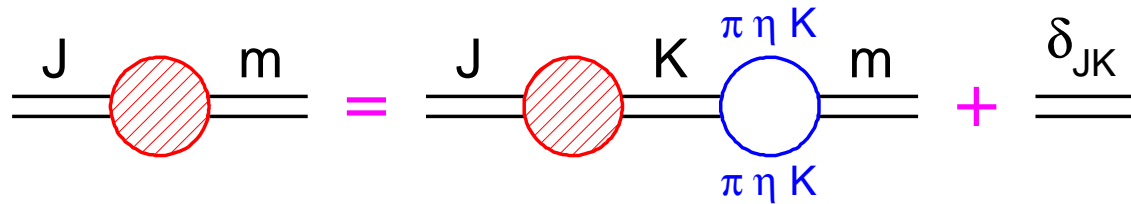
t,u-exchange subtraction procedure



t,u-exchange subtraction procedure



N/D based (D-matrix) analysis of the data



$$D_{jm} = D_{jk} \sum_{\alpha} B_{\alpha}^{km}(s) \frac{1}{M_m - s} + \frac{\delta_{jm}}{M_j^2 - s} \quad \hat{D} = \hat{\kappa}(I - \hat{B}\hat{\kappa})^{-1}$$

$$\hat{\kappa} = \text{diag} \left(\frac{1}{M_1^2 - s}, \frac{1}{M_2^2 - s}, \dots, \frac{1}{M_N^2 - s}, R_1, R_2 \dots \right)$$

$$\hat{B}_{ij} = \sum_{\alpha} B_{\alpha}^{ij} = \sum_{\alpha} \int \frac{ds'}{\pi} \frac{g_{\alpha}^{(R)i} \rho_{\alpha}(s', m_{1\alpha}, m_{2\alpha}) g_{\alpha}^{(L)j}}{s' - s - i0}$$

Pole parameters of the S_{11} states

	$N(1535)S_{11}$		$N(1650)S_{11}$		$N(1890)S_{11}$	
	K-matrix	D-matrix	K-matrix	D-matrix	K-matrix	D-matrix
M_{pole}	1501 ± 4	1494	1647 ± 6	1651	1900 ± 15	1905
Γ_{pole}	134 ± 11	116	103 ± 8	95	90^{+30}_{-15}	106
Elastic residue	31 ± 4	25	24 ± 3	23	1 ± 1	1.5
Phase	$-(29 \pm 5)^\circ$	-38°	$-(75 \pm 12)^\circ$	-62°	–	–
Res $\pi N \rightarrow N\eta$	28 ± 3	25	15 ± 3	15	4 ± 2	5
Phase	$-(76 \pm 8)^\circ$	-69°	$(132 \pm 10)^\circ$	140	$(40 \pm 20)^\circ$	42°
Res $\pi N \rightarrow \Delta\pi$	7 ± 4	4	11 ± 3	12	–	–
Phase	$(147 \pm 17)^\circ$	157°	$-(30 \pm 20)^\circ$	-40	–	–
$A^{1/2}$ ($\text{GeV}^{-\frac{1}{2}}$)	0.116 ± 0.010	0.107	0.033 ± 0.007	0.029	0.012 ± 0.006	0.010
Phase	$(7 \pm 6)^\circ$	1°	$-(9 \pm 15)^\circ$	0°	$120 \pm 50^\circ$	150°

Minimization methods

1. **The two body final states** $\pi N \rightarrow \pi N, \pi\pi \rightarrow \pi\pi, \gamma p \rightarrow \pi N, p\bar{p}(at\ rest) \rightarrow 3\pi$: χ^2 method. For n measured bins we minimize

$$\chi^2 = \sum_j^n \frac{(\sigma_j(PWA) - \sigma_j(exp))^2}{(\Delta\sigma_j(exp))^2}$$

2. **Reactions with three or more final states are analyzed with logarithm likelihood method. The minimization function:**

$$f = - \sum_j^{N(data)} \ln \frac{\sigma_j(PWA)}{\sum_m^{N(recMC)} \sigma_m(PWA)}$$

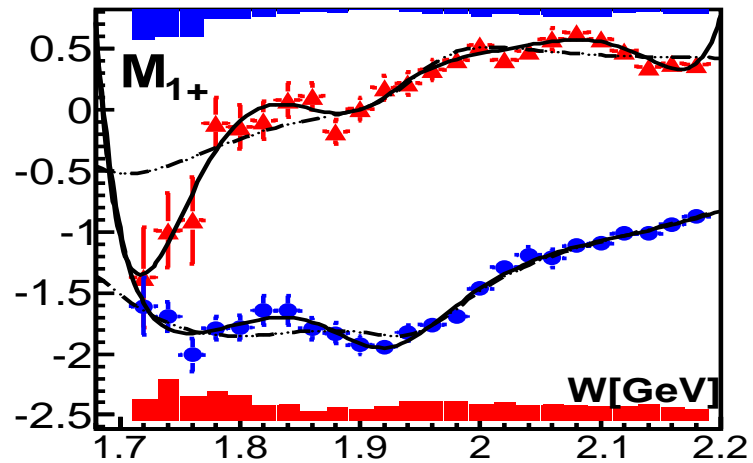
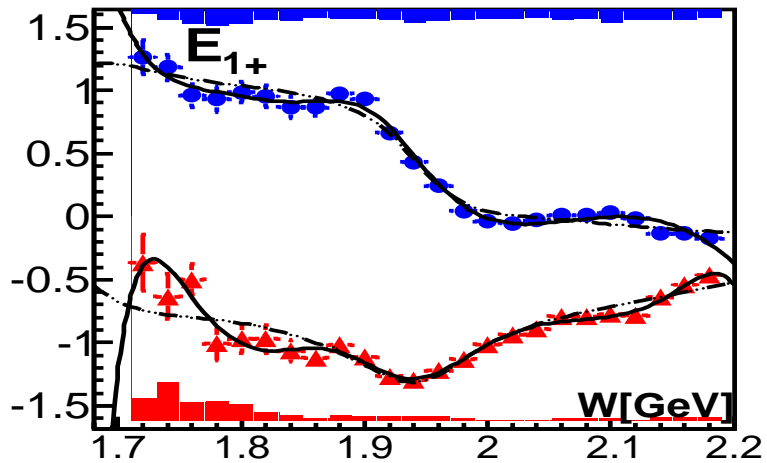
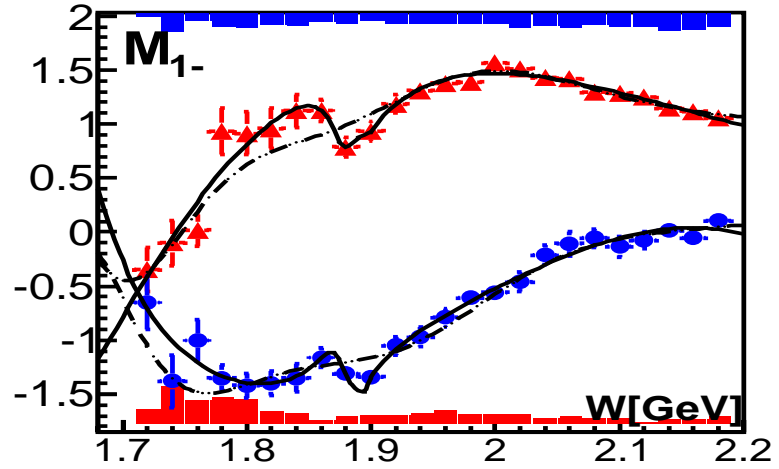
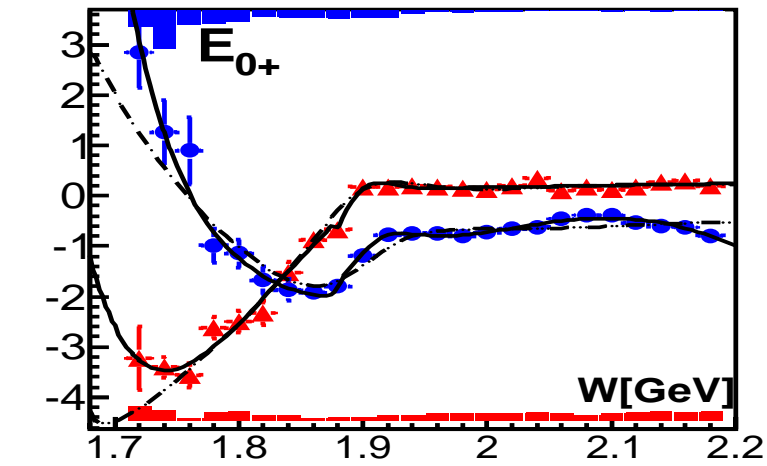
This method allows us to take into account all correlations in many dimensional phase space.

Recently included data

DATA	2011-2016	added in 2016-2018
$\gamma n \rightarrow \Lambda K, \Sigma^- K$		$\frac{d\sigma}{d\Omega}$ (CLAS), E (CLAS)
$\gamma n \rightarrow \pi^- p$	$\frac{d\sigma}{d\Omega}, \Sigma, P$	E (CLAS)
$\gamma n \rightarrow \eta n$	$\frac{d\sigma}{d\Omega}, \Sigma$	$\frac{d\sigma}{d\Omega}$ (MAMI) $\frac{d\sigma}{d\Omega} (h = \frac{1}{2})$ (CB-ELSA)
$\gamma p \rightarrow \eta p$	$\frac{d\sigma}{d\Omega}, \Sigma$ (GRAAL)	$\frac{d\sigma}{d\Omega}, F, T$ (MAMI) $T, P, H, G,$ (CB-ELSA) E, Σ (CB-ELSA, CLAS)
$\gamma p \rightarrow \eta' p$		$\frac{d\sigma}{d\Omega}, \Sigma$
$\gamma p \rightarrow K^+ \Lambda$	$\frac{d\sigma}{d\Omega}, \Sigma, P, T, C_x, C_z, O_{x'}, O_{z'}$	Σ, P, T, O_x, O_z (CLAS)
$\gamma p \rightarrow K^+ \Sigma^0$	$\frac{d\sigma}{d\Omega}, \Sigma, P, C_x, C_z$	Σ, P, T, O_x, O_z (CLAS)
$\pi^- p \rightarrow \pi^+ \pi^- n$		$d\sigma/d\Omega$ (HADES)
$\pi^- p \rightarrow \pi^- \pi^0 p$		$d\sigma/d\Omega$ (HADES)
$\gamma p \rightarrow \pi^0 \pi^0 p$	$d\sigma/d\Omega, \Sigma, E, I_c, I_s$	T, P, H, F, P_x, P_y (CB-ELSA)
$\gamma p \rightarrow \pi^+ \pi^- p$		$d\sigma/d\Omega, I_c, I_s$ (CLAS)
$\gamma p \rightarrow \omega p$	$d\sigma/d\Omega, \Sigma, \rho_{ij}^k, E, G$ (CB-ELSA)	Σ (CLAS) P, T, F, H (CLAS)
$\gamma p \rightarrow K^* \Lambda$		$d\sigma/d\Omega, \rho_{ij}$

Energy independent analysis of the $\gamma p \rightarrow K \Lambda$ reaction

Bonn-Gatchina-Tusla-Zagreb analysis

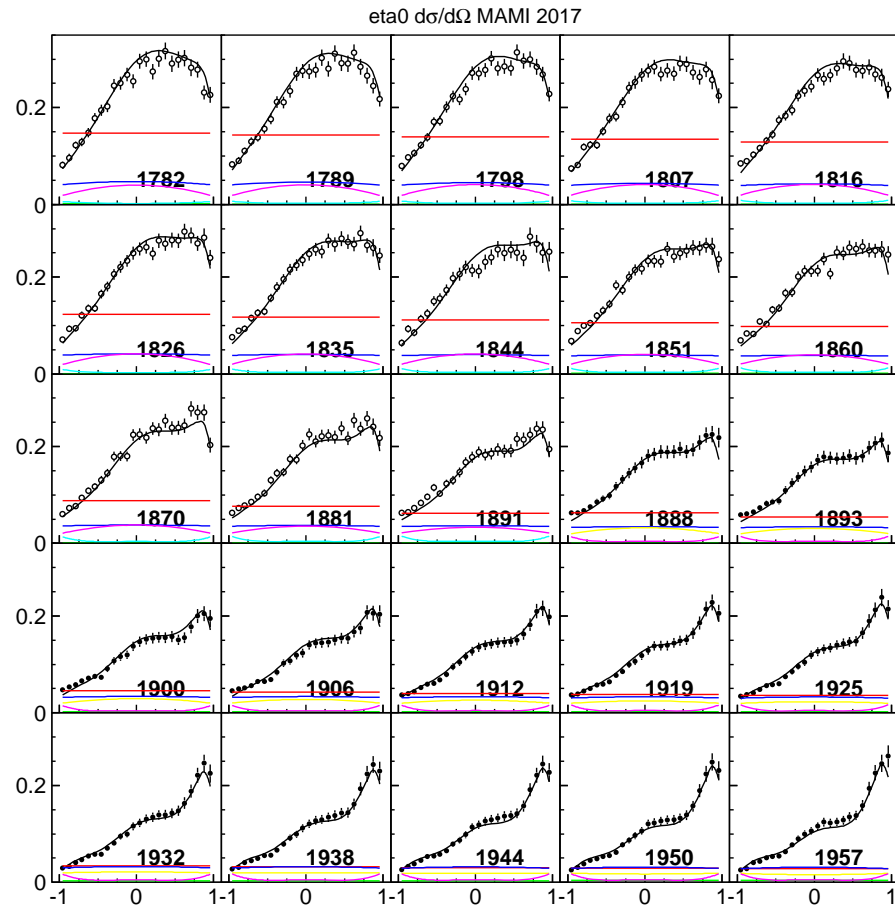
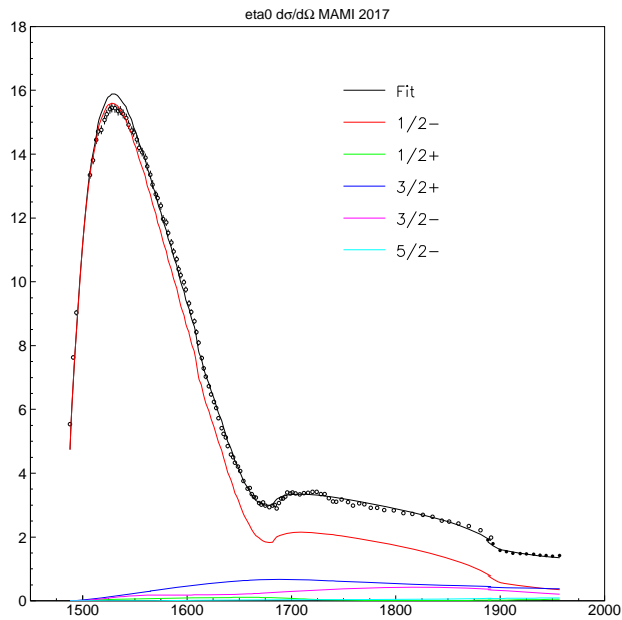


**The resonance parameters from the Bonn-Gatchina solution and from the analysis of
the energy-independent data**

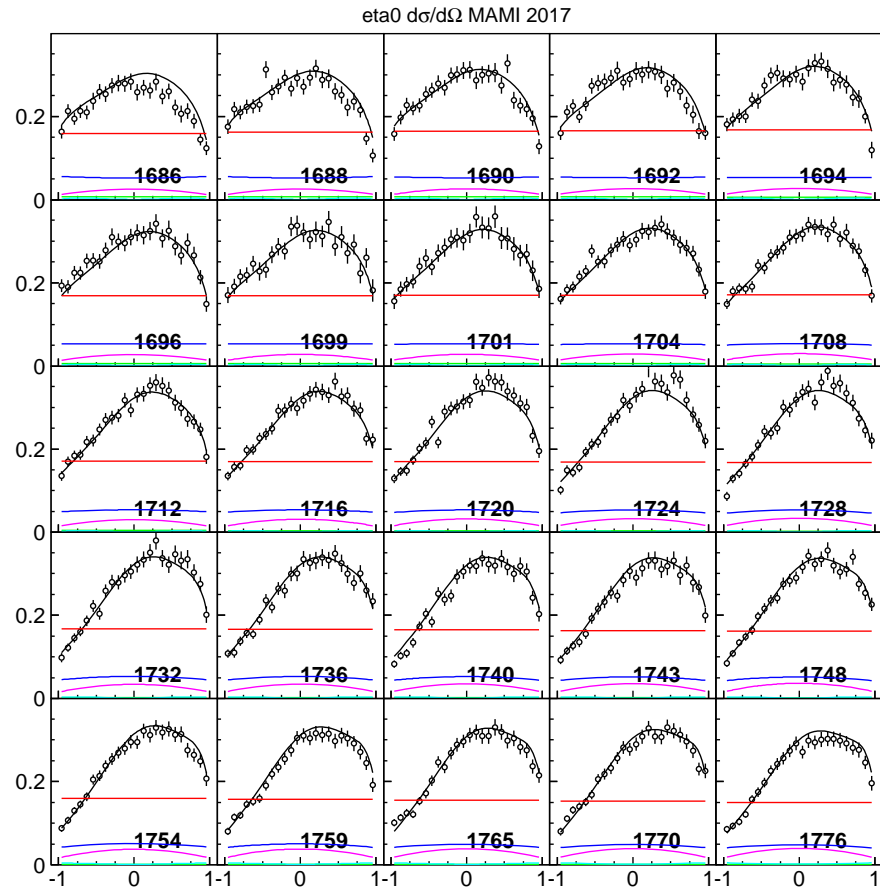
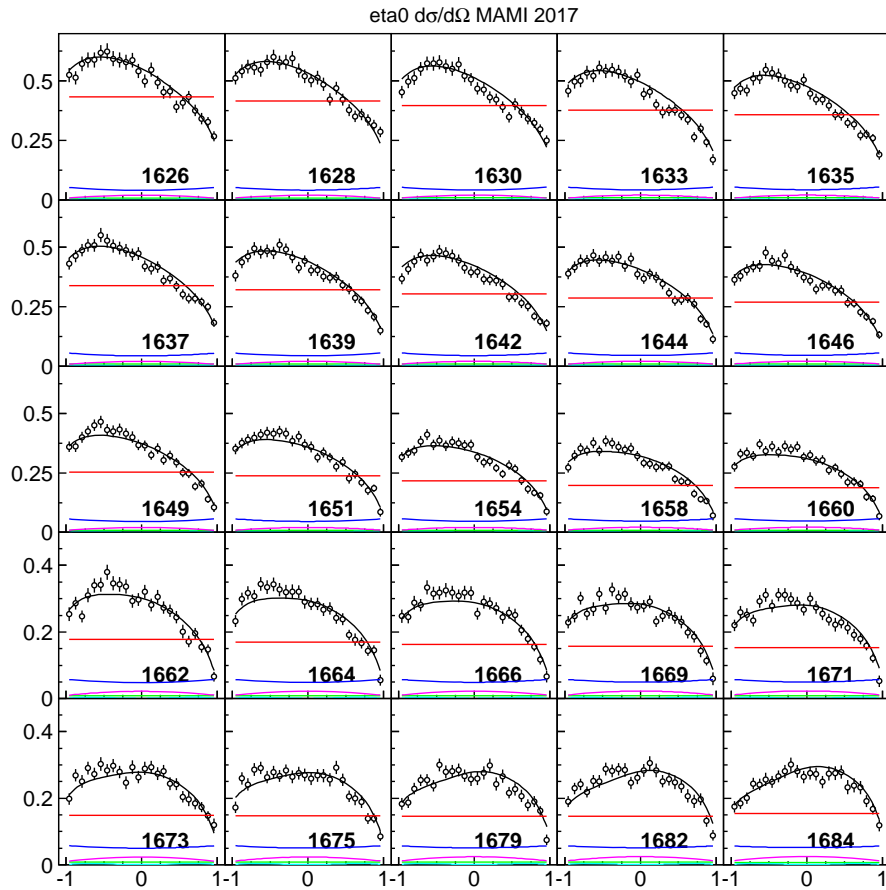
	$J^P = 1/2^-$		$J^P = 1/2^+$		$J^P = 3/2^+$	
	BnGa	L+P	BnGa	L+P	BnGa	L+P
M₁	1658 ± 10	1660 ± 5	1690 ± 15	1697 ± 23	-	-
Γ_1	102 ± 8	59 ± 16	155 ± 25	84 ± 34	-	-
$ Res $	0.26 ± 0.10	0.10 ± 0.10	0.16 ± 0.05	$0.12^{+0.24}_{-0.12}$	-	-
Θ_1	$(110 \pm 20)^0$	$(95 \pm 33)^0$	$-(160 \pm 25)^0$	$-(119 \pm 83)^0$	-	-
M₂	1895 ± 15	1906 ± 17	1860 ± 40	1875 ± 11	1945 ± 35	1912 ± 30
Γ_2	132 ± 30	100 ± 10	230 ± 50	33 ± 9	235^{+70}_{-30}	166 ± 30
$ Res $	0.09 ± 0.03	0.06 ± 0.02	0.05 ± 0.02	0.30 ± 0.10	0.03 ± 0.02	—
Θ_2	$(8 \pm 30)^0$	$(87 \pm 27)^0$	$(27 \pm 30)^0$	$(82 \pm 9)^0$	$(90 \pm 40)^0$	—

The analysis of the new $\gamma p \rightarrow \eta p$ data.

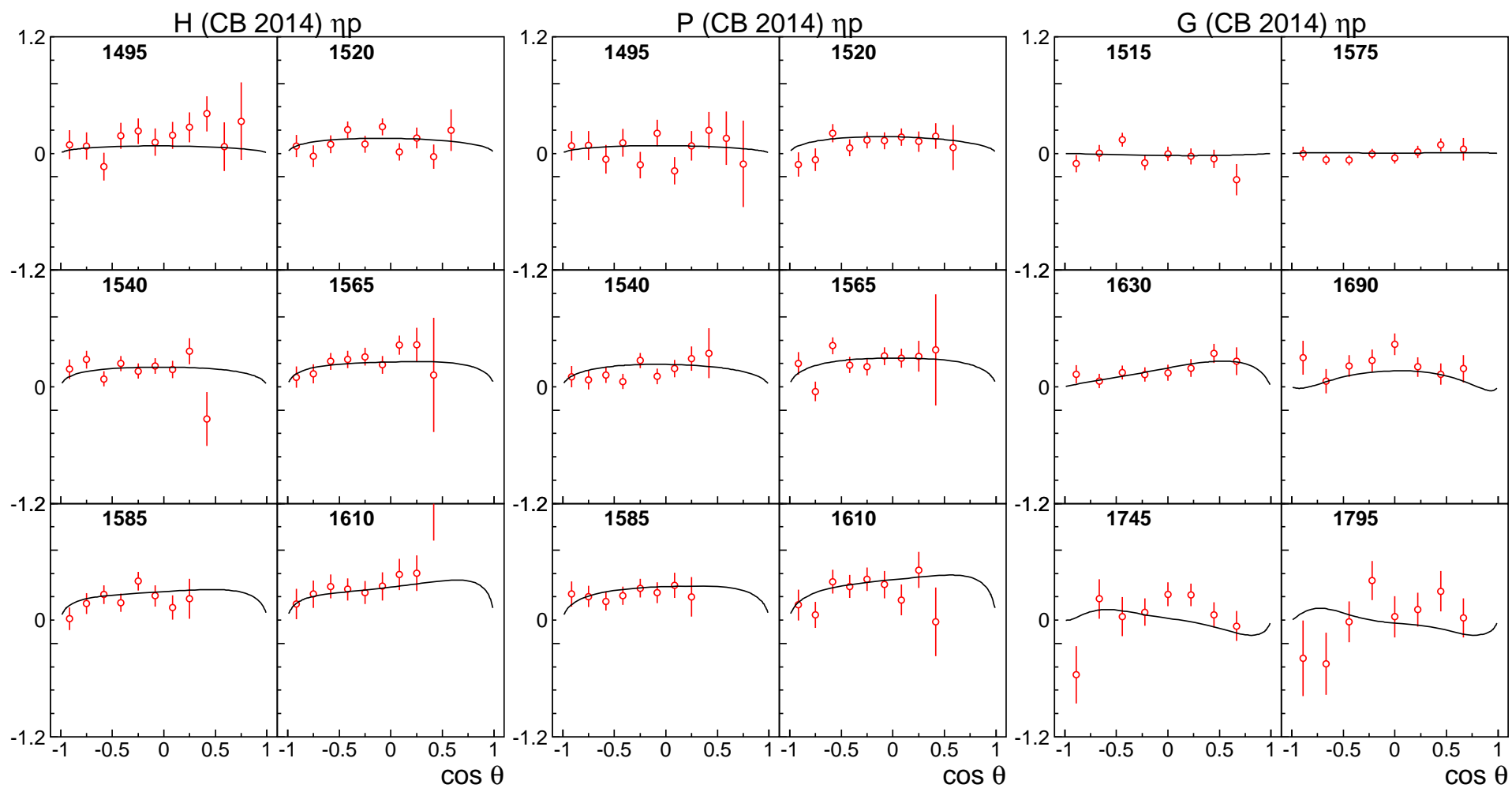
New MAMI data: a strong cusp effect from the $\eta' p$ channel



The analysis of the new $\gamma p \rightarrow \eta p$ data. $d\sigma/d\Omega$ (MAMI)

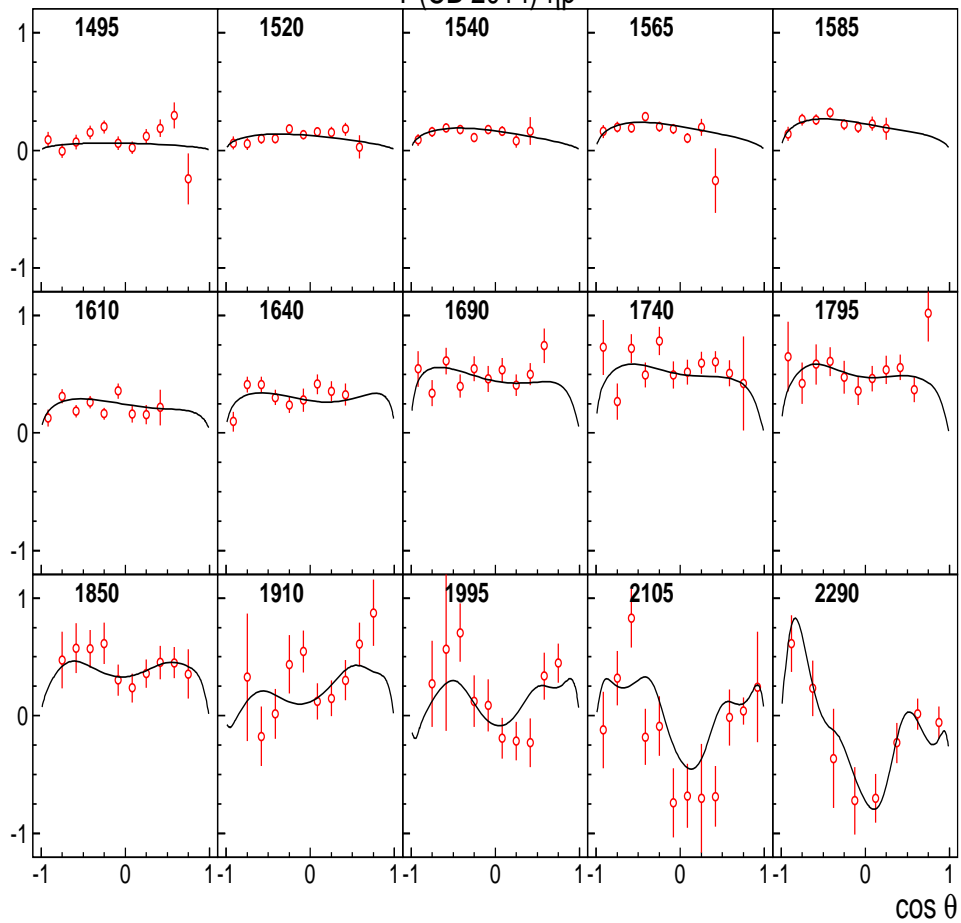


The analysis of the new $\gamma p \rightarrow \eta p$ data. H, P, T (CB-ELSA)

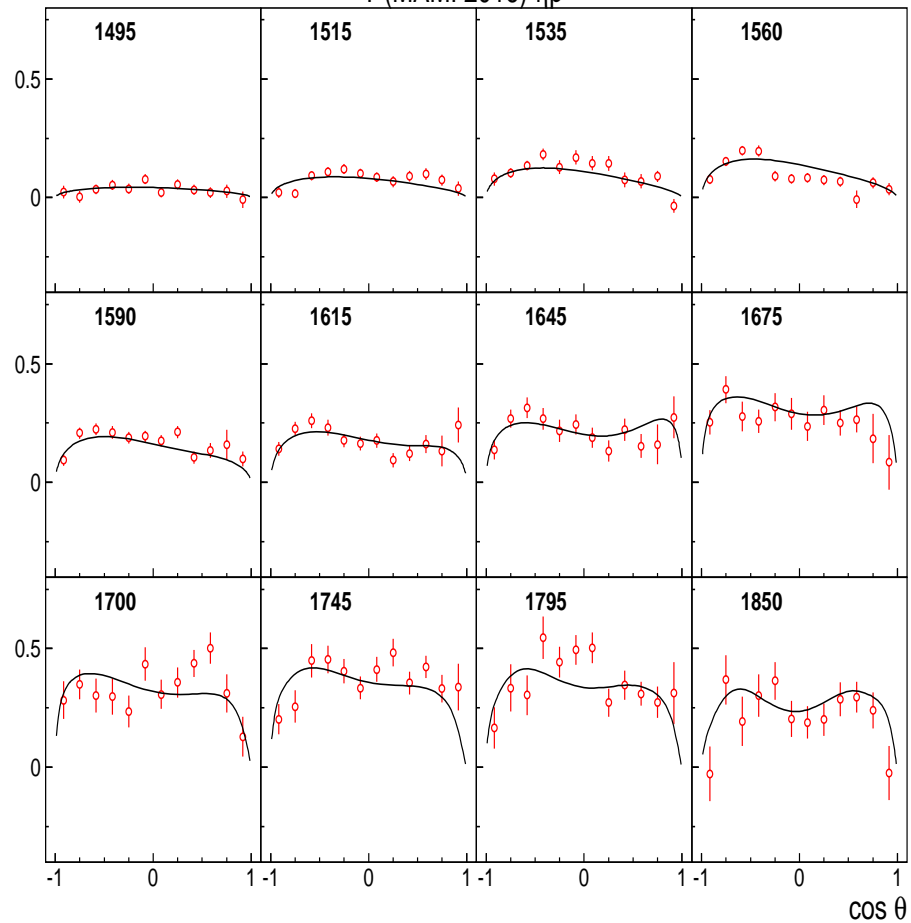


The analysis of the new $\gamma p \rightarrow \eta p$ data. T (CB-ELSA), (MAMI scale 1.4)

T (CB 2014) ηp

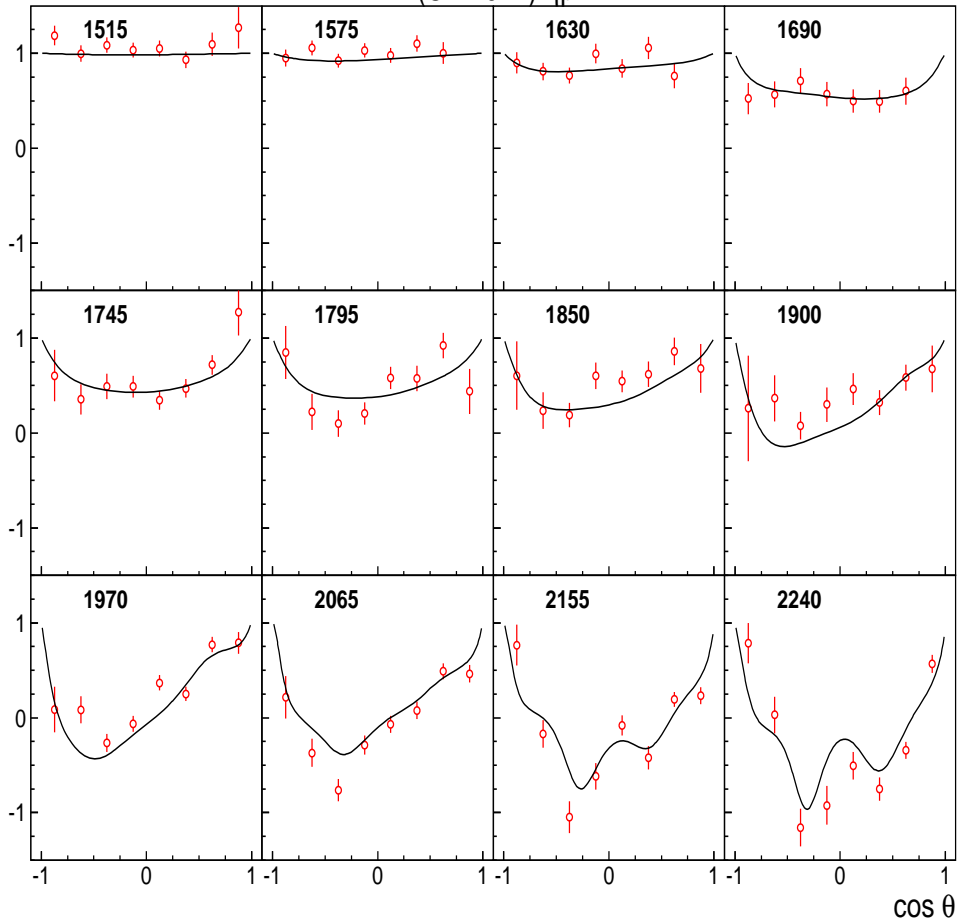


T (MAMI 2016) ηp

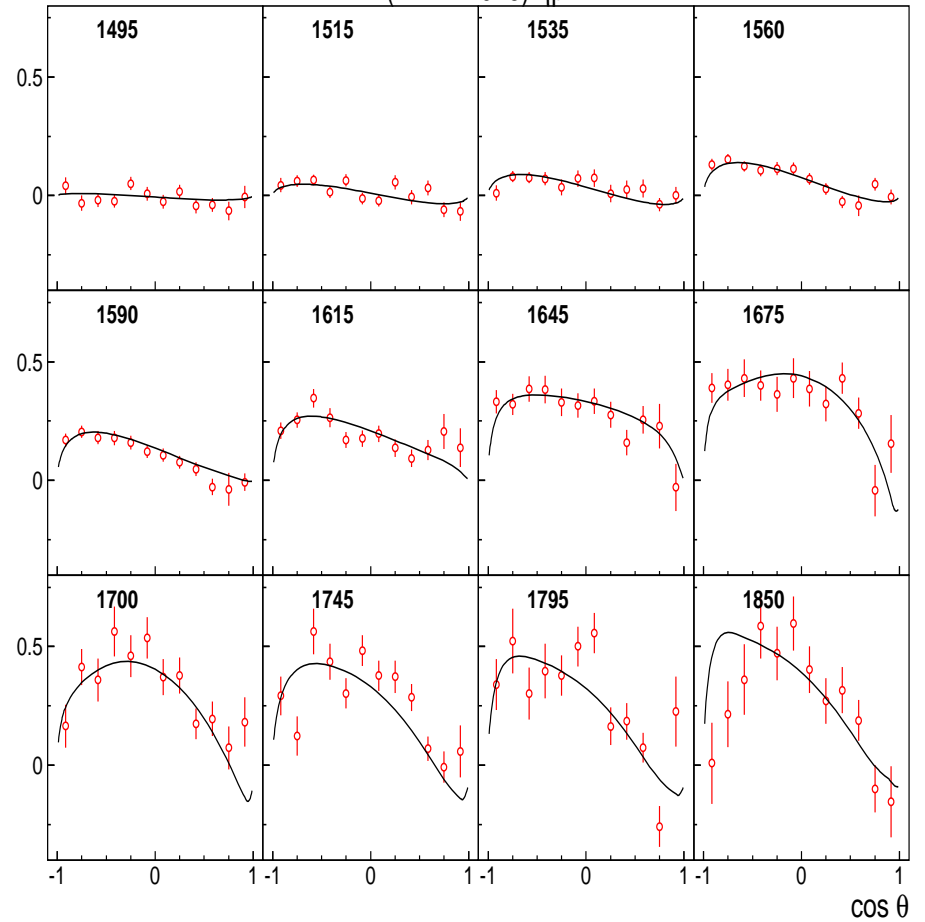


The analysis of the new $\gamma p \rightarrow \eta p$ data. E (CB-ELSA), F (MAMI) (scale 1.4)

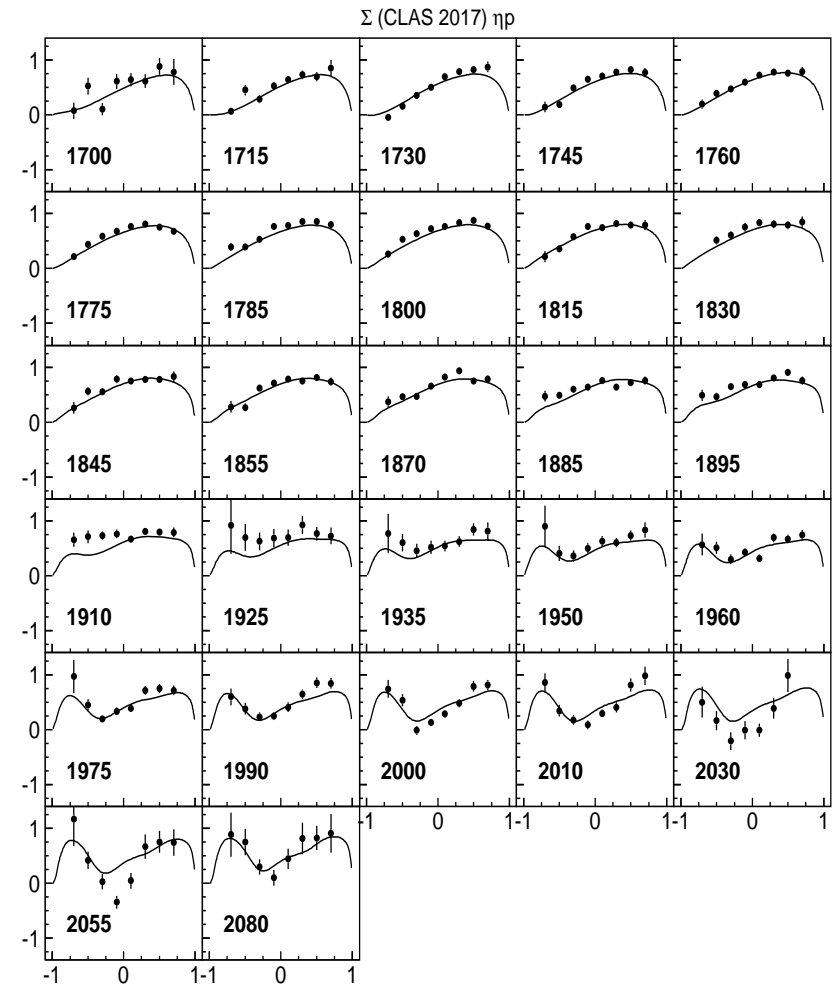
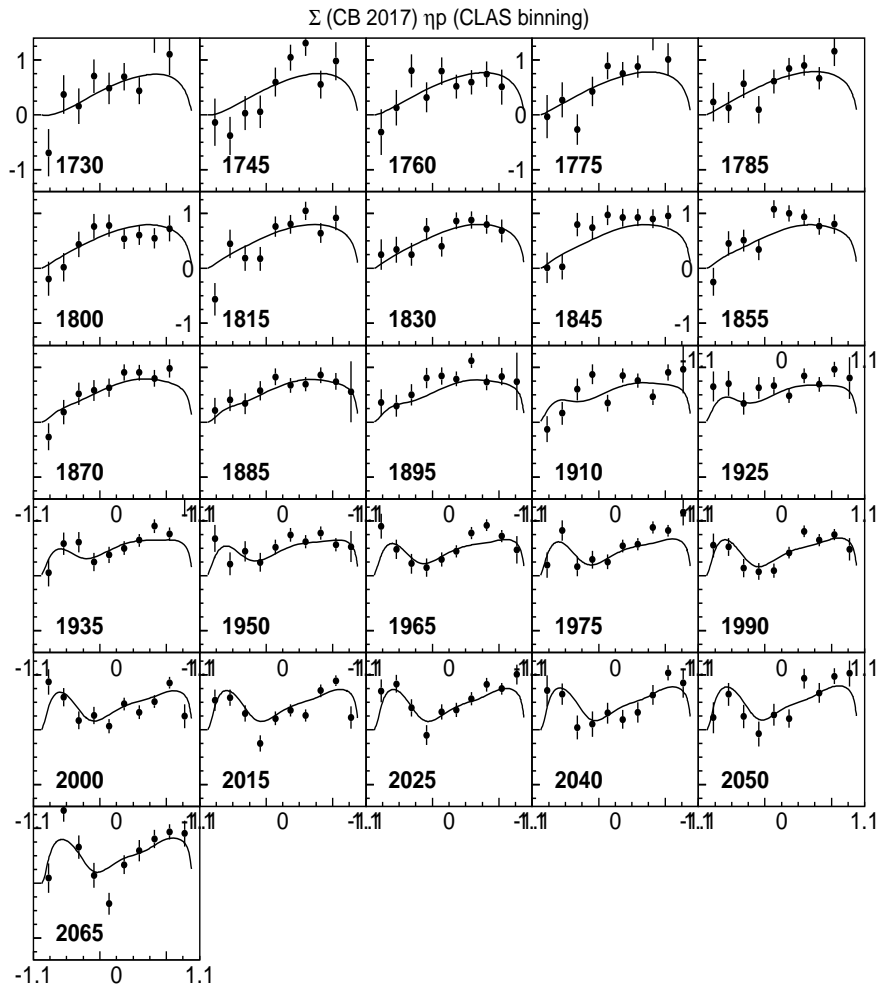
E (CB 2017) ηp



F (MAMI 2016) ηp



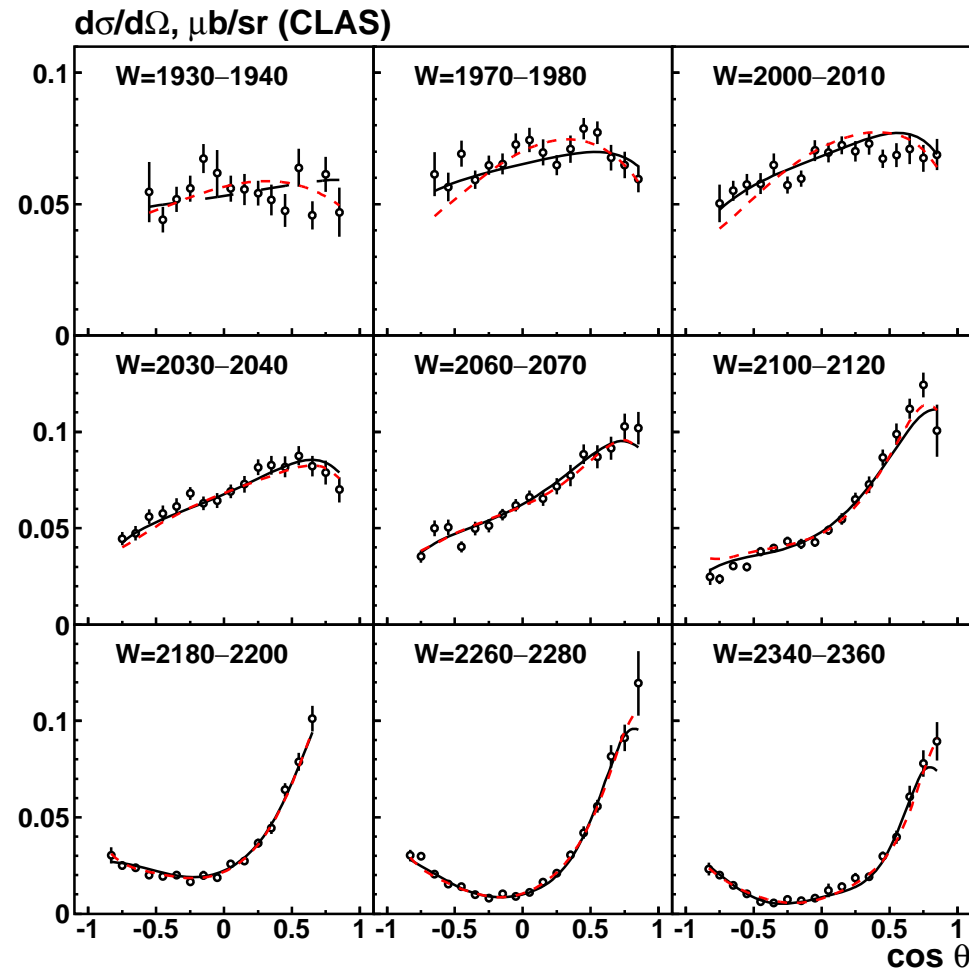
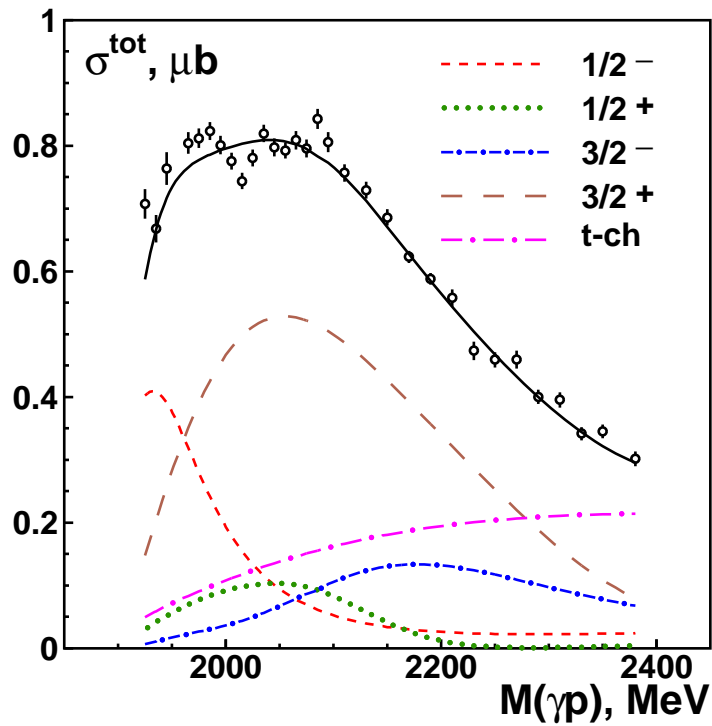
The analysis of the new $\gamma p \rightarrow \eta p$ data. Σ (CB-ELSA and CLAS)



Resonance branchings to the ηN channel

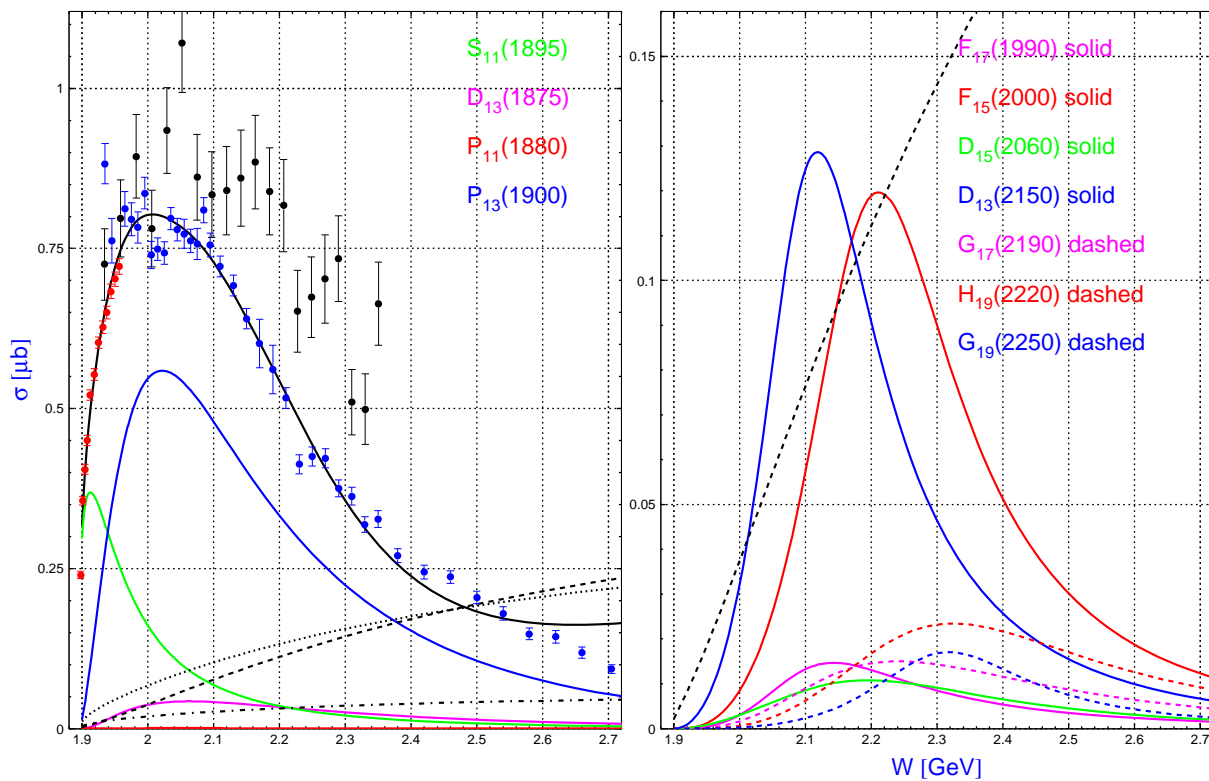
Res.	BR	Res.	BR	Res.	BR
$N(1535)$ $1/2^-$	0.42 ± 0.04 0.42 ± 0.10	$N(1650)$ $1/2^-$	0.32 ± 0.04 $0.05 - 0.15$	$N(1895)$ $1/2^-$	0.10 ± 0.05 (0.21 ± 0.06)
$N(1710)$ $1/2^+$	0.25 ± 0.09 $0.10 - 0.30$	$N(1880)$ $1/2^+$	0.19 ± 0.07 $(0.25^{+0.30}_{-0.20})$	$N(2100)$ $1/2^+$	0.25 ± 0.10 0.61 ± 0.61
$N(1520)$ $3/2^-$	< 0.001 0.0023 ± 0.0004	$N(1700)$ $3/2^-$	0.01 ± 0.01 0 ± 0.01	$N(1875)$ $3/2^-$	0.02 ± 0.01 0.012 ± 0.018
$N(1720)$ $3/2^+$	0.03 ± 0.02 0.021 ± 0.014	$N(1900)$ $3/2^+$	0.03 ± 0.01 ~ 0.12	$N(2120)$ $3/2^-$	≤ 0.01 -
$N(1675)$ $5/2^-$	0.005 ± 0.005 0 ± 0.007	$N(2060)$ $5/2^-$	0.04 ± 0.01 0.04 ± 0.02	$N(2190)$ $7/2^-$	0.025 ± 0.005 0 ± 0.01
$N(1680)$ $5/2^+$	0.002 ± 0.001 0 ± 0.007	$N(2000)$ $5/2^+$	0.002 ± 0.001 0.002 ± 0.002	$N(1990)$ $7/2^+$	≤ 0.01 -

The analysis of the $\gamma p \rightarrow \eta' p$ data.



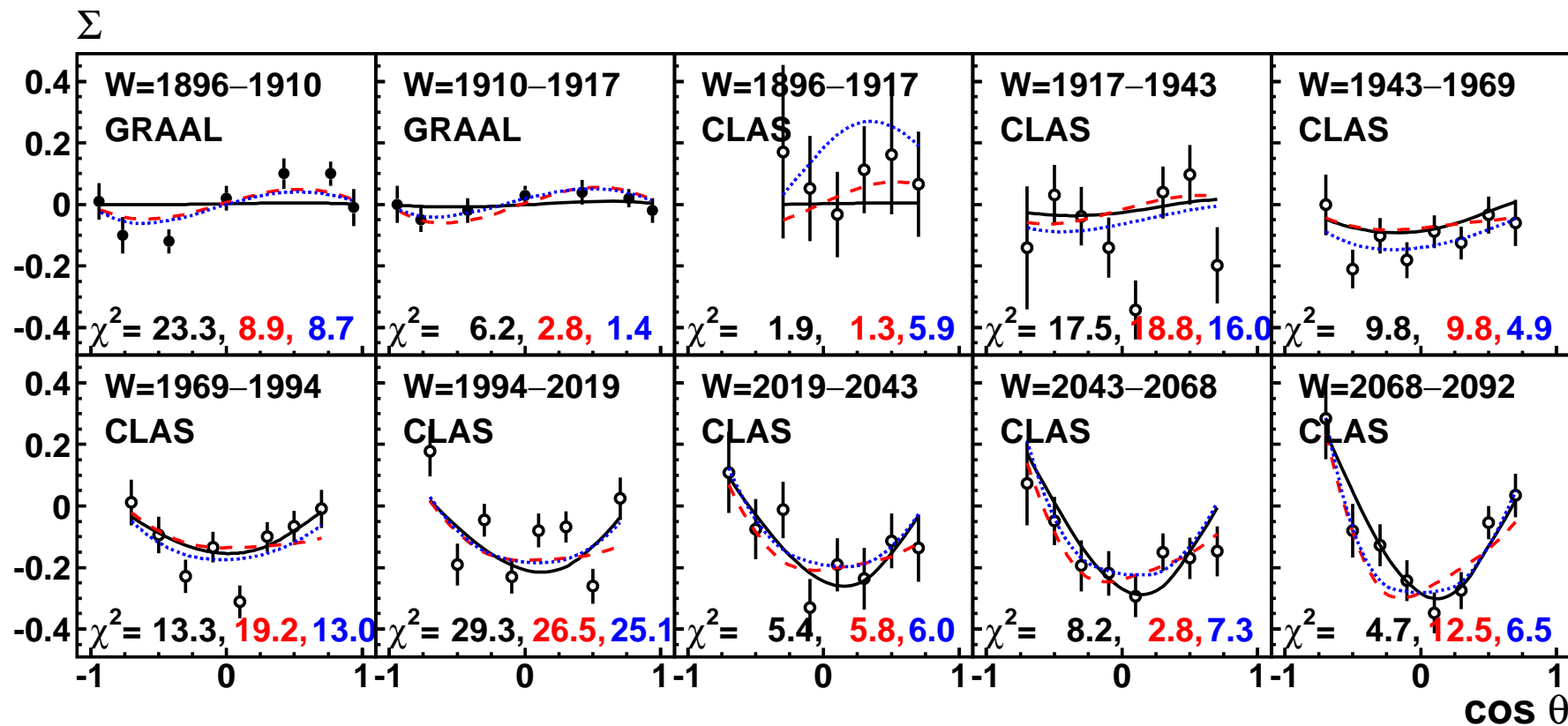
Strong contribution from the $S_{11}(1895)$, $P_{13}(1900)$, $P_{11}(2100)$ and $D_{13}(2120)$ states.

MAID analysis of the new $\gamma p \rightarrow \eta' p$ data



	Bonn-Gatchina	MAID
Mass (MeV)	1895 ± 15	1896 ± 1
Width (MeV)	90^{+30}_{-15}	93 ± 13

The beam asymmetry on $\gamma p \rightarrow \eta' p$

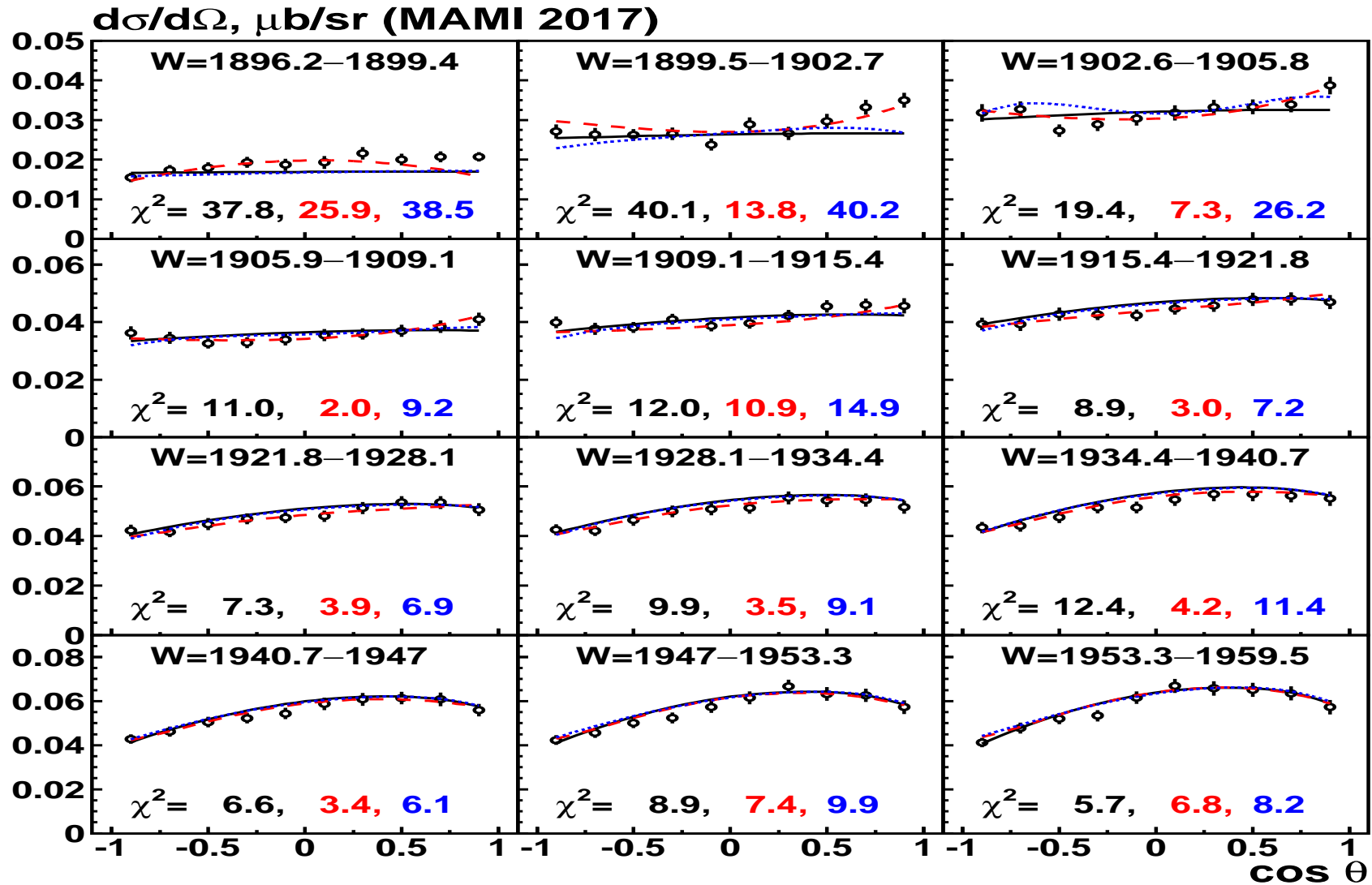


No narrow states

$D_{15}(1903)$

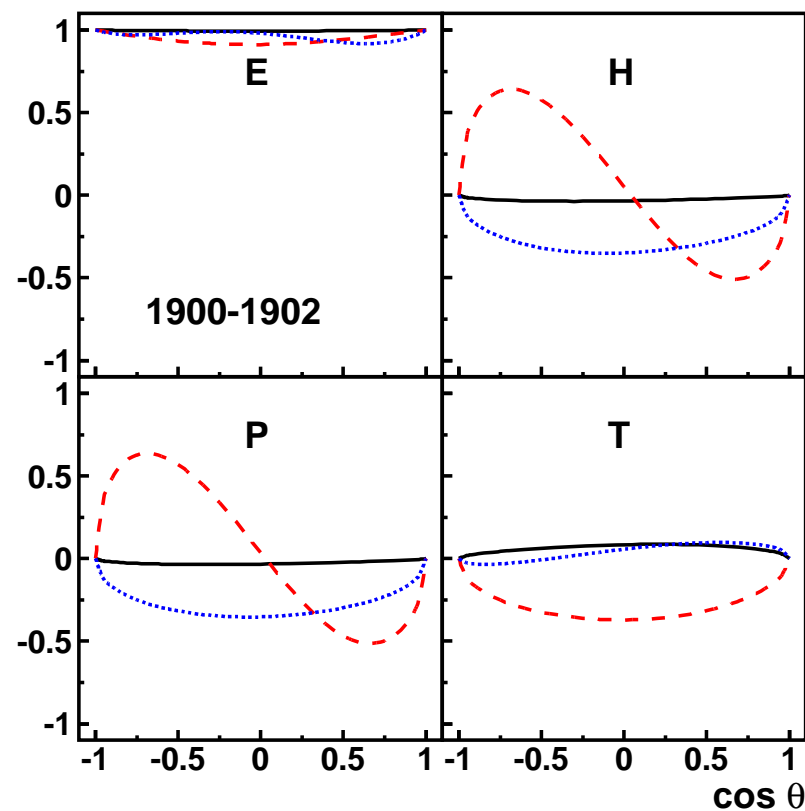
$D_{13}(1900)$

The differential cross section from MAMI on $\gamma p \rightarrow \eta' p$

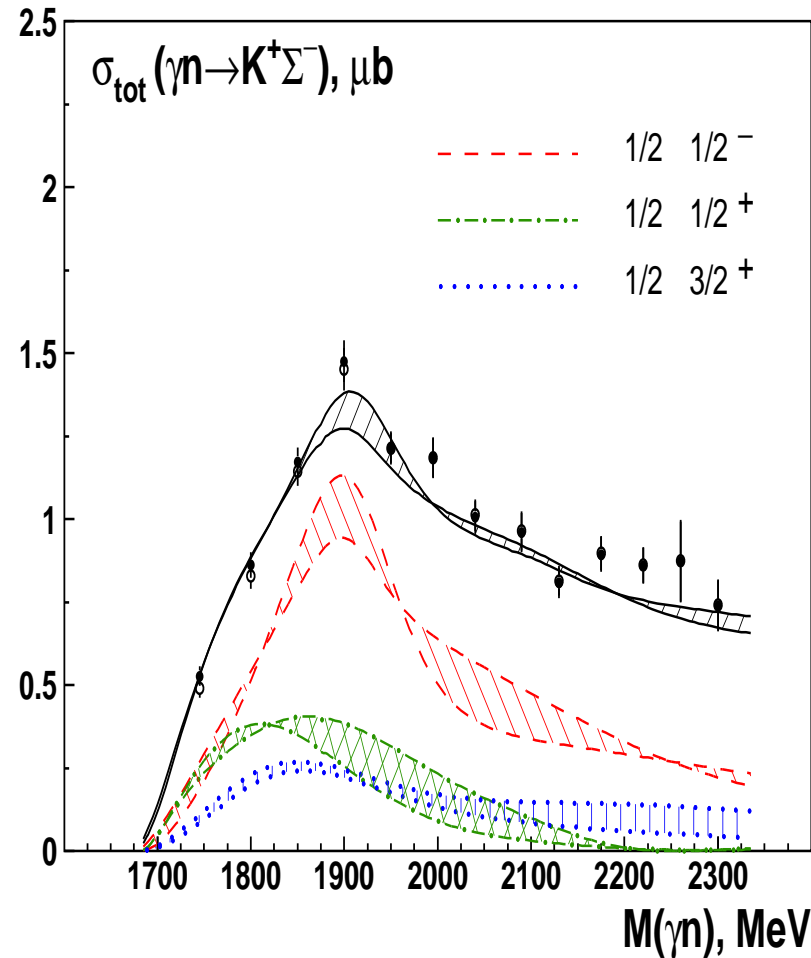
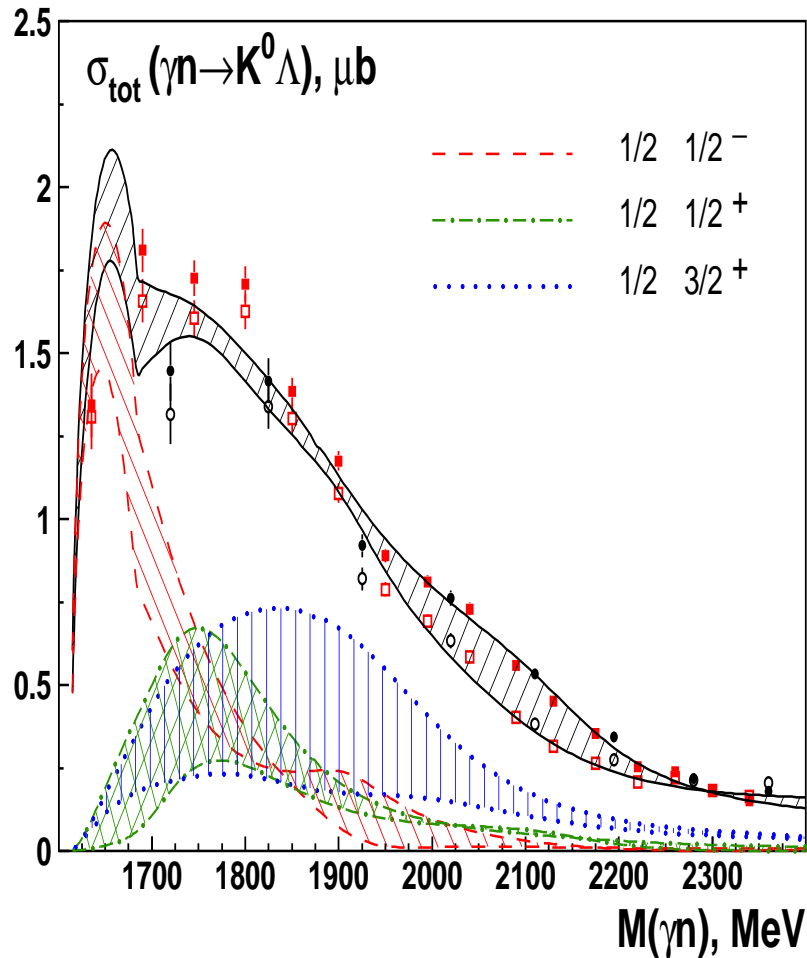


The description of the data below $W=1917$ MeV and the prediction of other observables

Resonance	N	Basic	D_{13}	D_{15}
M (MeV)			1900	1903
Γ (MeV)			1	1
χ^2 (Σ)	13	29.5	11.7	10.1
χ^2 ($\frac{d\sigma}{d\Omega}$)	50	120.3	59.9	129.0

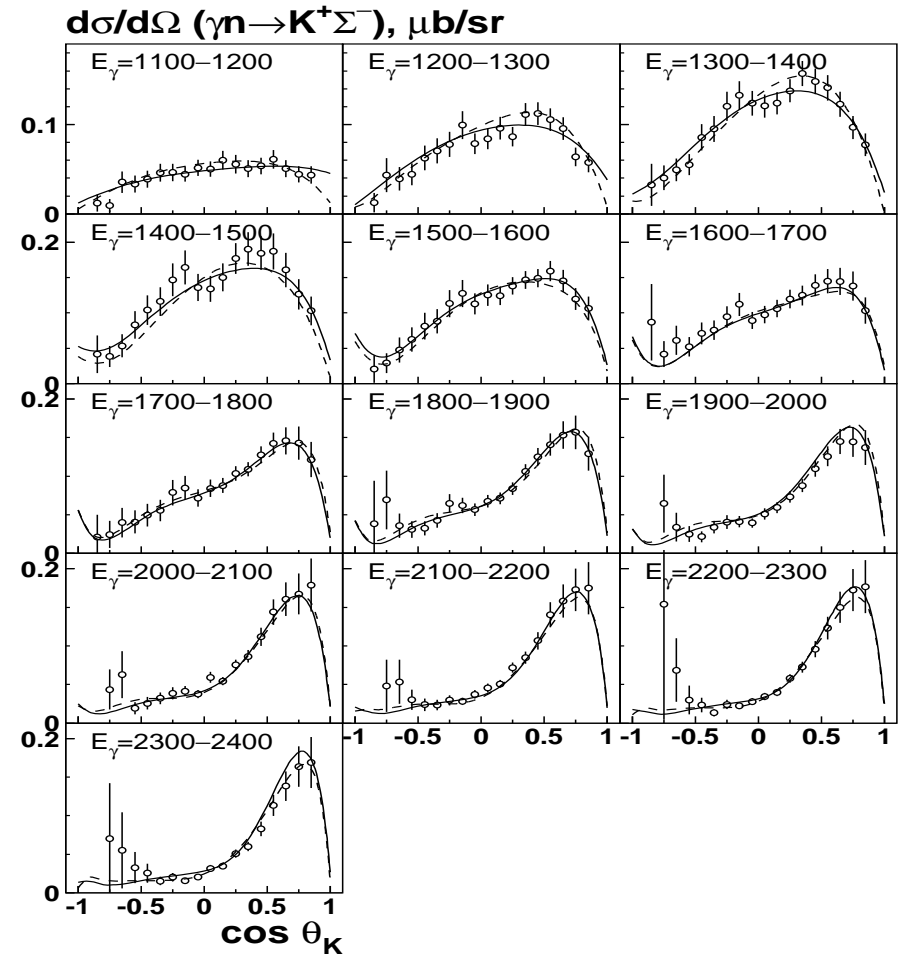
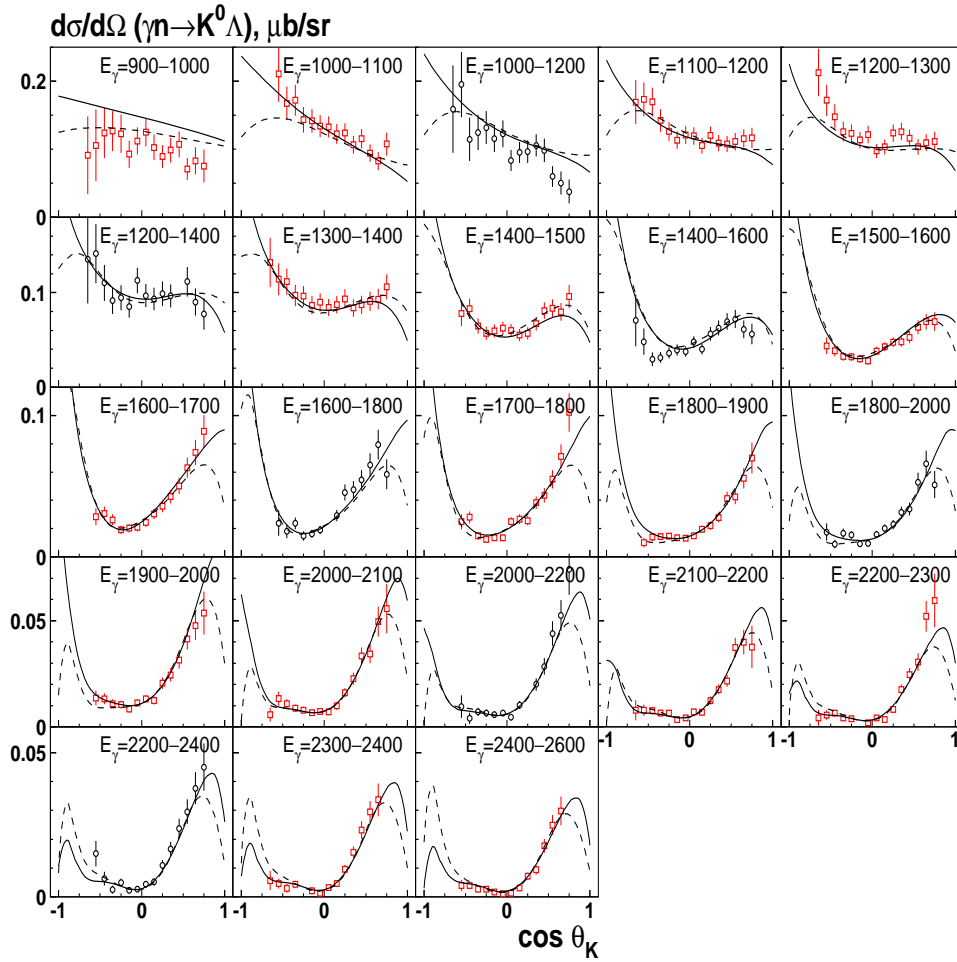


The analysis of the $\gamma n \rightarrow K \Lambda$ data and the $\gamma n \rightarrow K^+ \Sigma^-$ data (Practically no free parameters)



Clear contributions from the $S_{11}(1895)$ and $P_{13}(1900)$ states.

Description of the differential cross section



New CLAS data on the helicity asymmetry $\gamma n \rightarrow K^+ \Sigma^-$

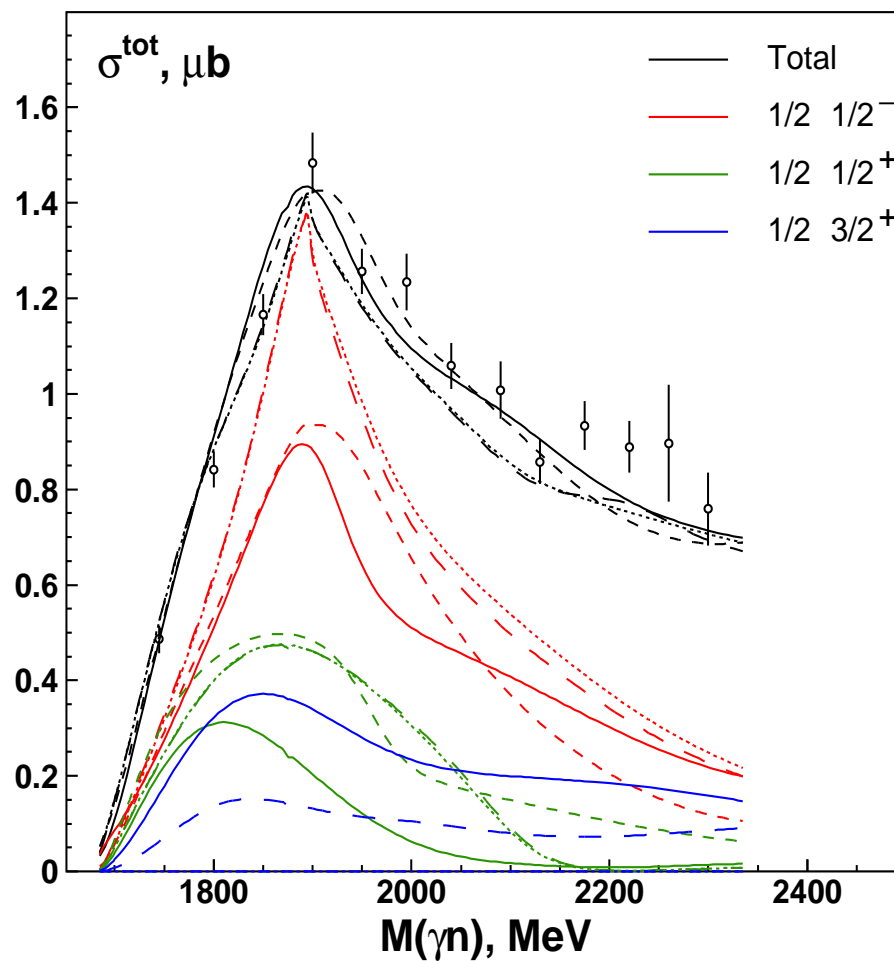
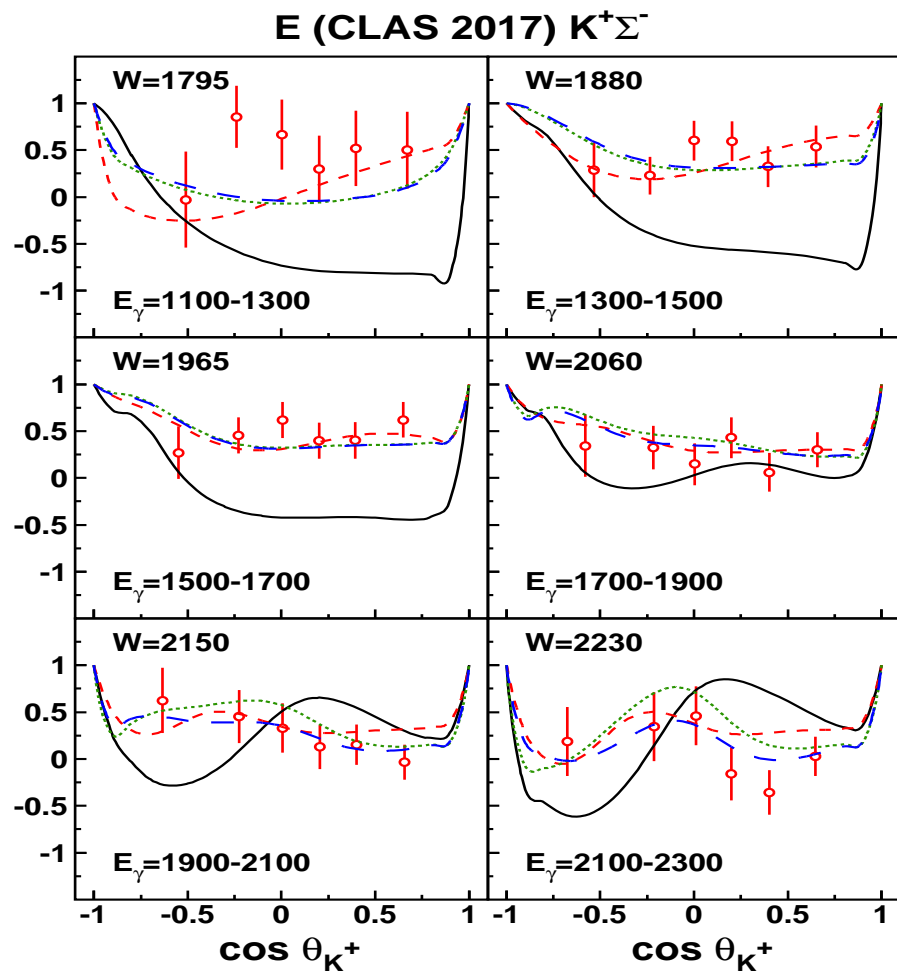


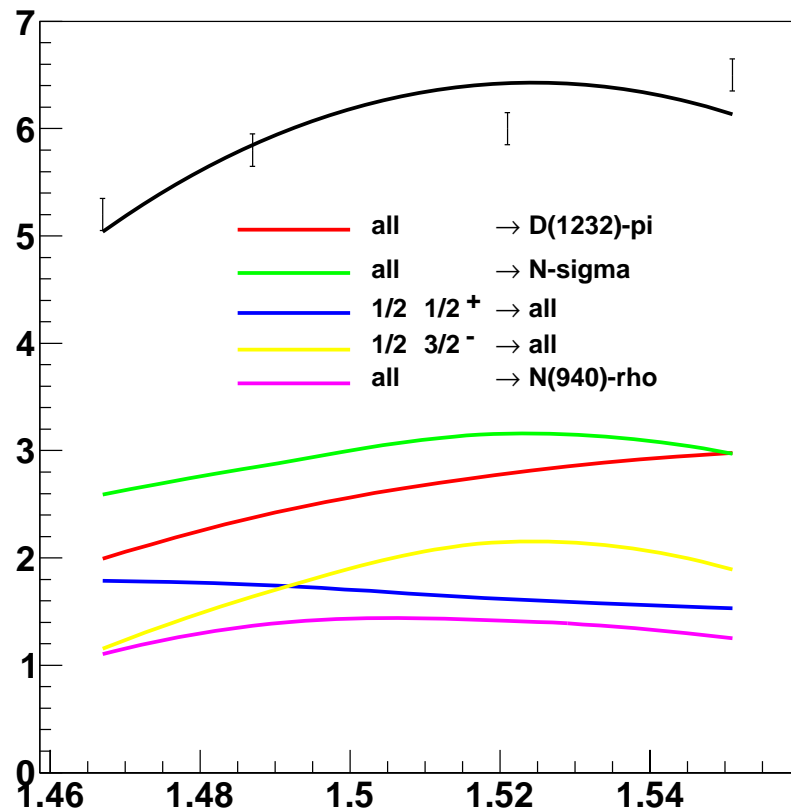
Table 1: The γN couplings ($\text{GeV}^{-1/2}10^{-3}$) at the pole position

	$A_{1/2}$	Phase	$A_{3/2}$	Phase
$N(1535)1/2^-$	-88 ± 4	$5 \pm 4^\circ$		
$N(1650)1/2^-$	16 ± 4	$-28 \pm 10^\circ$		
$N(1895)1/2^-$	-15 ± 10	$60 \pm 25^\circ$		
$N(1440)1/2^+$	41 ± 5	$23 \pm 10^\circ$		
$N(1710)1/2^+$	29 ± 7	$80 \pm 20^\circ$		
$N(1880)1/2^+$	72 ± 24	$-30 \pm 30^\circ$		
$N(2100)1/2^+$	29 ± 9	$35 \pm 20^\circ$		
$N(1520)3/2^-$	-45 ± 5	$-5 \pm 4^\circ$	-119 ± 5	$5 \pm 4^\circ$
$N(1875)3/2^-$	4 ± 3	$-85 \pm 35^\circ$	-6 ± 4	$-85 \pm 45^\circ$
$N(2120)3/2^-$	80 ± 30	$15 \pm 25^\circ$	-33 ± 20	$-60 \pm 35^\circ$
$N(1720)3/2^+$	$-(25_{-15}^{+40})$	$-75 \pm 35^\circ$	100 ± 35	$-80 \pm 35^\circ$
$N(1900)3/2^+$	-98 ± 20	$-13 \pm 20^\circ$	74 ± 15	$5 \pm 15^\circ$
$N(1975)3/2^+$	-26 ± 13	$8 \pm 25^\circ$	-77 ± 15	$5 \pm 20^\circ$
$N(1675)5/2^-$	-53 ± 4	$-3 \pm 5^\circ$	-73 ± 5	$-12 \pm 5^\circ$
$N(2060)5/2^-$	52 ± 25	$-5 \pm 20^\circ$	12 ± 7	$-40 \pm 35^\circ$
$N(1680)5/2^+$	32 ± 3	$-7 \pm 5^\circ$	-63 ± 4	$-10 \pm 5^\circ$
$N(2000)5/2^+$	19 ± 10	$-80 \pm 40^\circ$	11 ± 5	$82 \pm 30^\circ$
$N(1990)7/2^+$	-32 ± 15	$5 \pm 20^\circ$	-70 ± 25	$0 \pm 20^\circ$
$N(2190)7/2^-$	30 ± 7	$5 \pm 15^\circ$	-23 ± 8	$13 \pm 20^\circ$

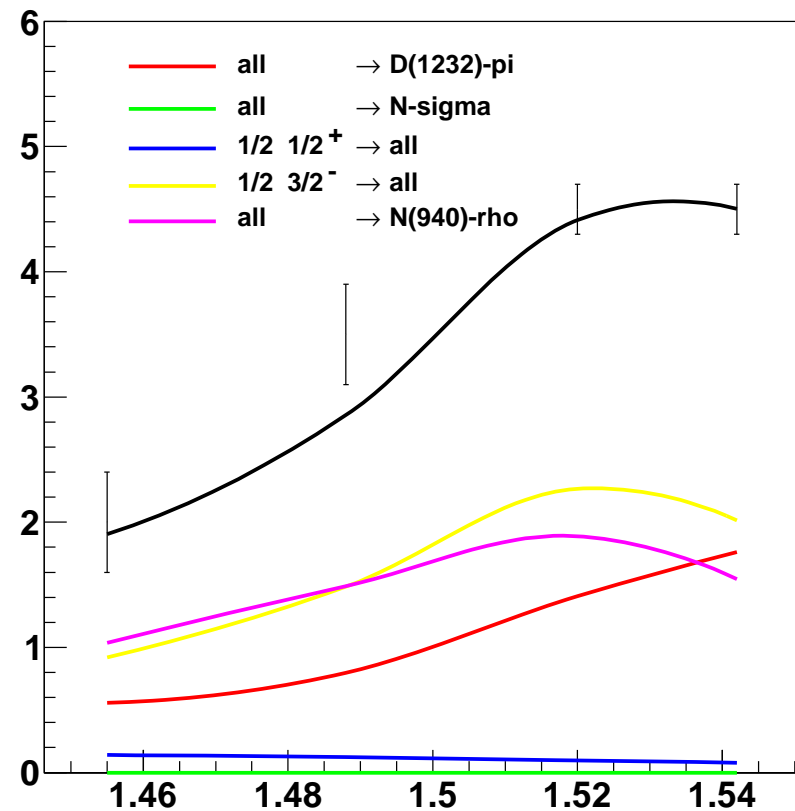
The total cross section from the HADES data

$\pi^- p \rightarrow \pi^+ \pi^- n$ and $\pi^- p \rightarrow \pi^- \pi^0 p$ data (W.Przigoda)

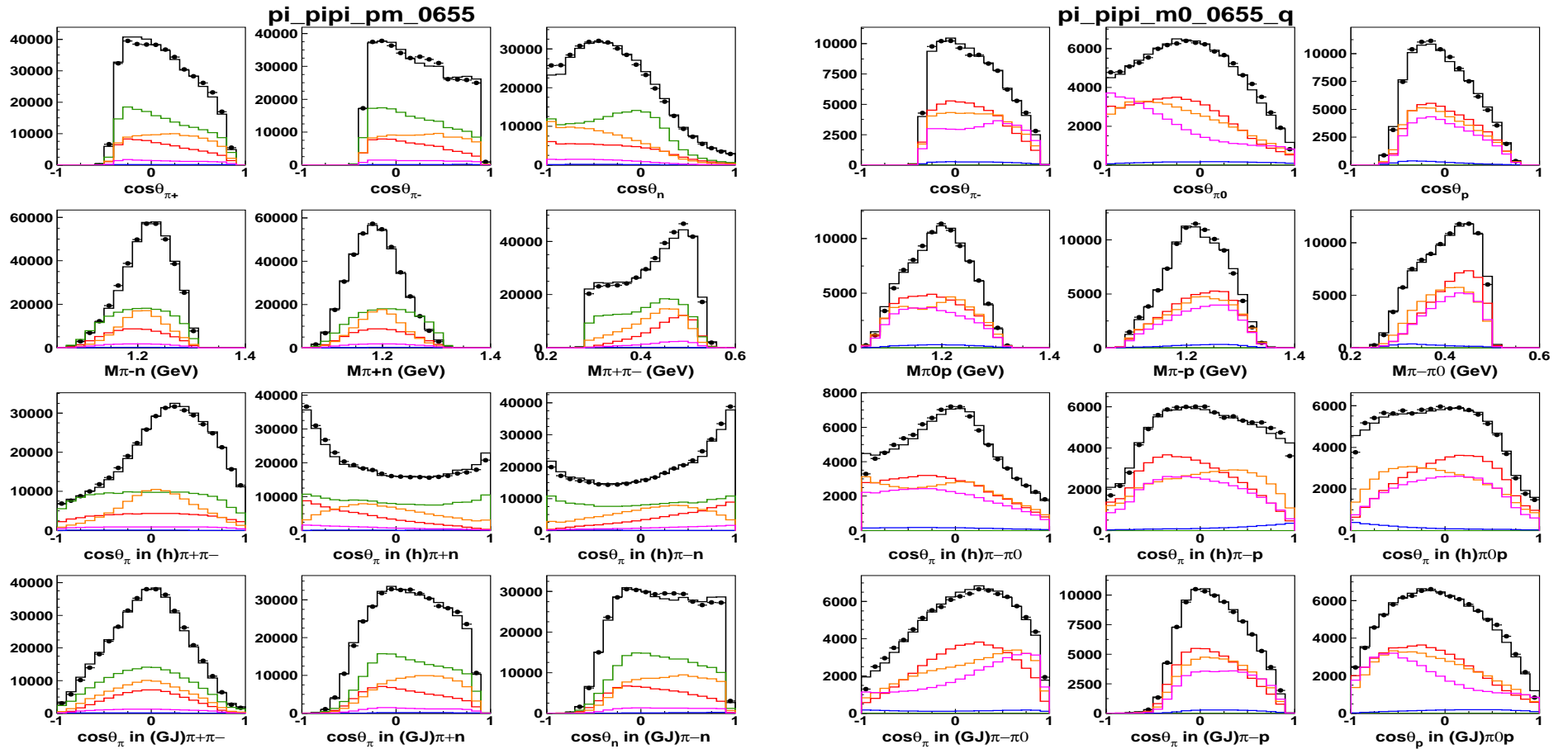
Graph



Graph



HADES data on $\pi^- p \rightarrow \pi^+ \pi^- n$ and $\pi^- \pi^0 p$ at P=656 MeV/c (W.Przigoda) (Preliminary)



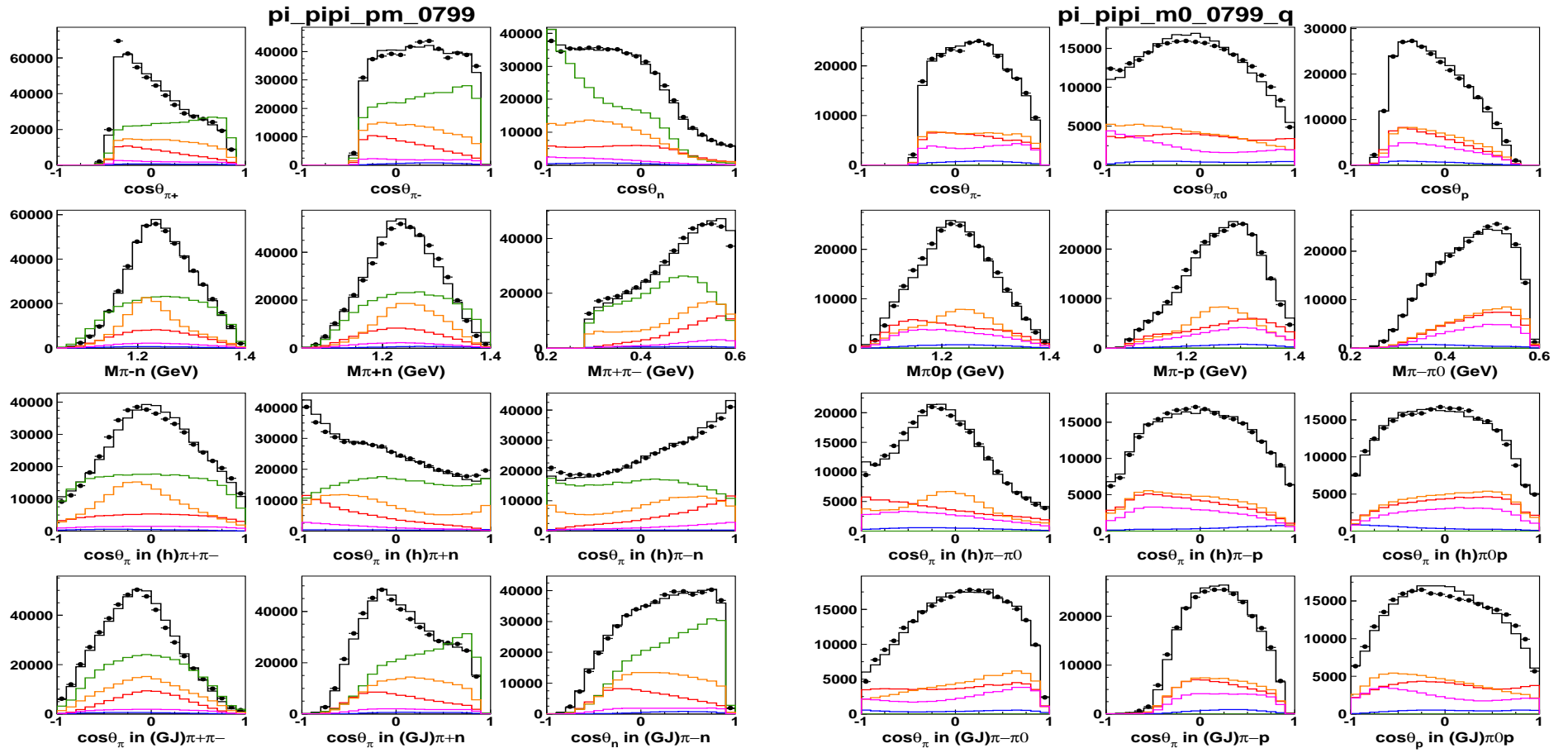
— $\Delta(1232)\pi$

— $N\sigma$

— $\rho N(940)$

— $\frac{1}{2} \frac{3}{2}^-$

HADES data on $\pi^- p \rightarrow \pi^+ \pi^- n$ and $\pi^- \pi^0 p$ at P=656 MeV/c (W.Przigoda) (Preliminary)



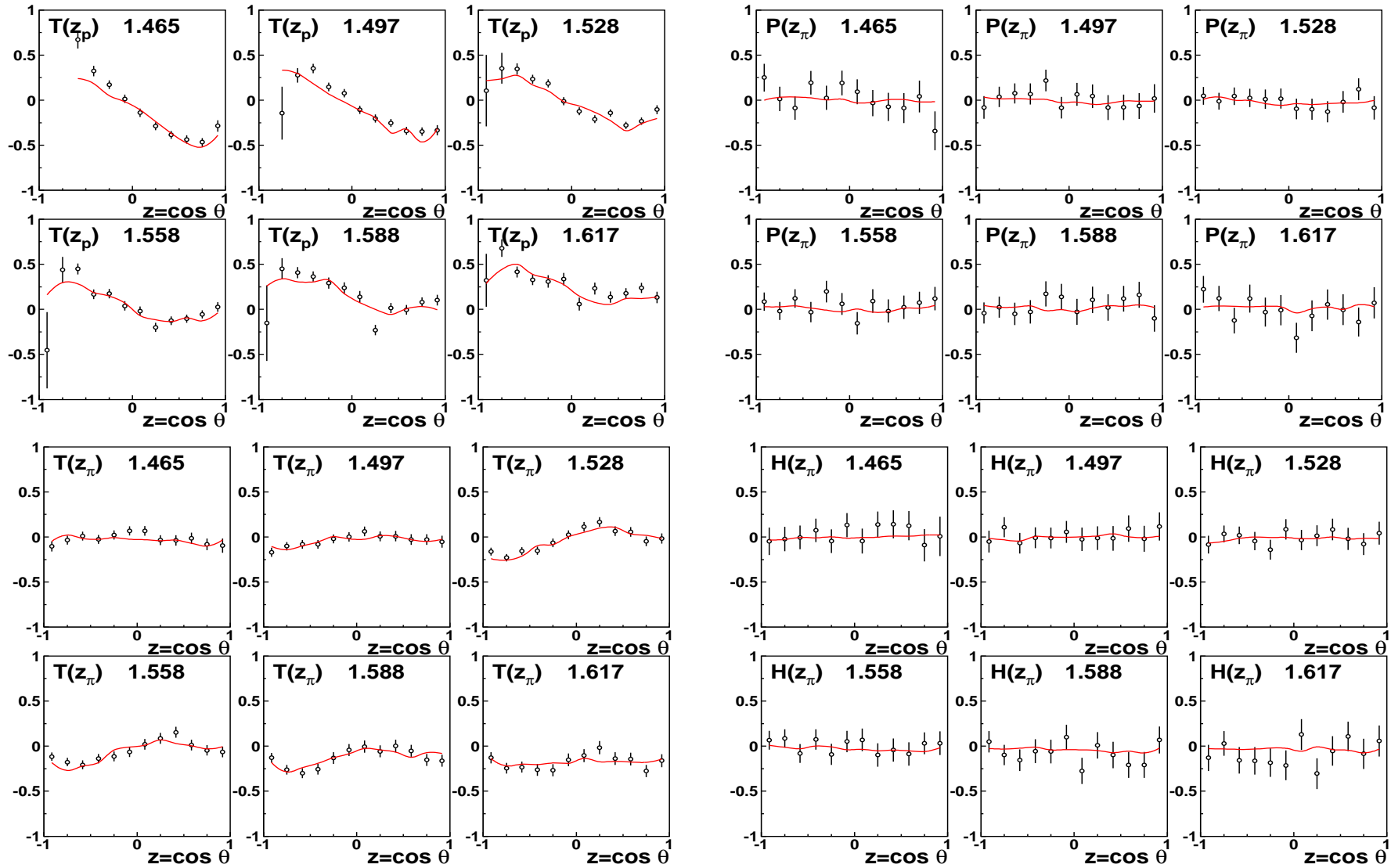
— $\Delta(1232)\pi$

— $N\sigma$

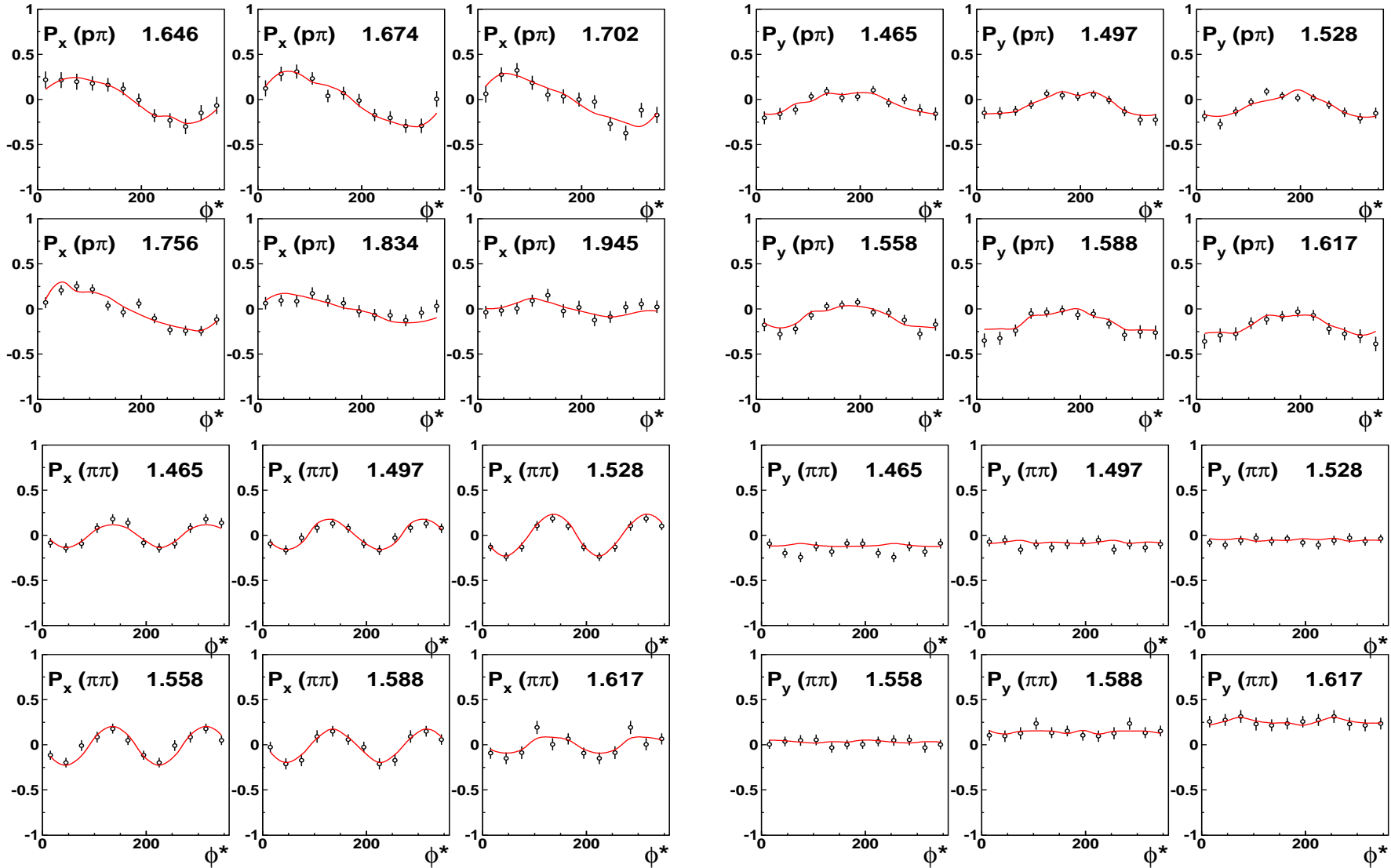
— $\rho N(940)$

— $\frac{1}{2} \frac{3}{2}^-$

Fit of the H, P, T ($\gamma p \rightarrow \pi^0 \pi^0 p$) from CB-ELSA (T. Seifen, Preliminary)



Fit of the P_x, P_y, P_x^S, P_y^S observables ($\gamma p \rightarrow \pi^0 \pi^0 p$) from CB-ELSA (T. Seifen, Preliminary)



$N_{\rho(770)}$ branching ratio (Preliminary)

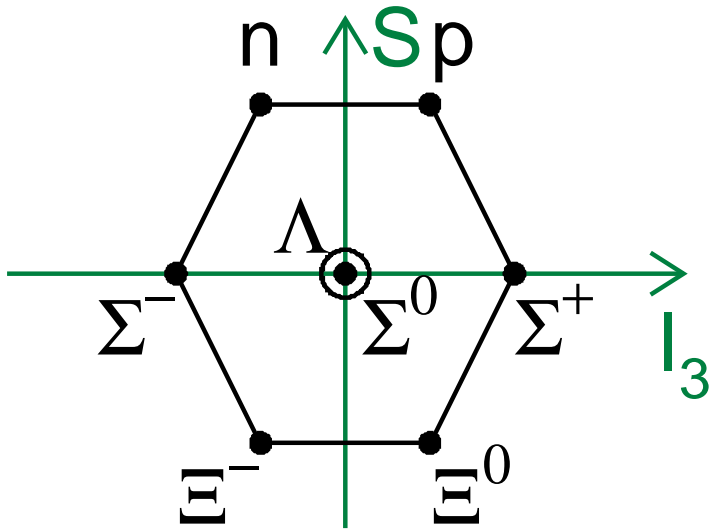
$N(1440)1/2^+$	<1%	$N(1520)3/2^-$	$12 \pm 2\%$	$N(1535)1/2^-$	$2 \pm 1\%$
$N(1650)1/2^-$	$13 \pm 2\%$	$N(1675)5/2^-$	<1%	$N(1685)5/2^+$	$12 \pm 2\%$
$N(1710)1/2^+$	$9 \pm 3\%$	$N(1720)3/2^+$	$60 \pm 18\%$	$N(1880)1/2^+$	$30 \pm 8\%$
$N(1895)1/2^-$	$55 \pm 10\%$	$N(1875)3/2^-$	$60 \pm 14\%$	$N(2060)5/2^-$	$12 \pm 8\%$
$N(2120)3/2^-$	$50 \pm 17\%$	$N(2000)5/2^+$	$20 \pm 12\%$	$N(1900)3/2^+$	$25 \pm 10\%$
$\Delta(1600)3/2^+$	$2 \pm 2\%$	$\Delta(1620)1/2^-$	$40 \pm 5\%$	$\Delta(1940)3/2^+$	$8 \pm 4\%$
$\Delta(2200)3/2^+$	$20 \pm 8\%$	$\Delta(1700)3/2^-$	$12 \pm 4\%$	$\Delta(2100)3/2^-$	$11 \pm 5\%$
$\Delta(1750)1/2^+$	$40 \pm 12\%$	$\Delta(1900)1/2^-$	$30 \pm 8\%$	$\Delta(1905)5/2^+$	$35 \pm 8\%$

0.1 N^* and Δ spectrum

Resonance	Rating	N_{pp}	Resonance	Rating	N_{pp}	Resonance	Rating	N_{pp}
N(1440)1/2 ⁺	****	13	N(1520)3/2 ⁻	****	17	N(1535)1/2 ⁻	****	15
N(1650)1/2 ⁻	****	18	N(1675)5/2 ⁻	****	14	N(1680)5/2 ⁺	****	17
N(1685)	*		N(1700)3/2 ⁻	***	15	N(1710)1/2 ⁺	***	14
N(1720)3/2 ⁺	****	17	N(1860)5/2 ⁺	**	9	N(1875)3/2 ⁻	***	16
N(1880)1/2 ⁺	**	20	N(1895)1/2 ⁻	**	17	N(1900)3/2 ⁺	***	18
N(1990)7/2 ⁺	**	9	N(2000)5/2 ⁺	**	11	N(2040)3/2 ⁺	*	
N(2060)5/2 ⁻	**	13	N(2100)1/2 ⁺	*		N(2150)3/2 ⁻	**	11
N(2190)7/2 ⁻	****	11	N(2220)7/2 ⁻	****	7	N(2250)9/2 ⁻	****	
N(2600)11/2 ⁻	***		N(2700)13/2 ⁺	**				
Δ (1232)	****	8	Δ (1600)3/2 ⁺	***	12	Δ (1620)1/2 ⁻	****	10
Δ (1700)3/2 ⁻	****	11	Δ (1750)1/2 ⁺	*		Δ (1900)1/2 ⁻	**	13
Δ (1905)5/2 ⁺	****	11	Δ (1910)1/2 ⁺	****	13	Δ (1920)3/2 ⁺	***	21
Δ (1930)5/2 ⁻	***		Δ (1940)3/2 ⁻	*	5	Δ (1950)7/2 ⁺	****	13
Δ (2000)5/2 ⁺	**		Δ (2150)1/2 ⁻	*		Δ (2200)7/2 ⁻	*	
Δ (2300)9/2 ⁺	**		Δ (2350)3/2 ⁻	*		Δ (2390)7/2 ⁺	*	
Δ (2420)11/2 ⁺	****		Δ (2400)9/2 ⁻	****		Δ (2750)13/2 ⁻	**	
Δ (2950)15/2 ⁺	**							

$$3 \otimes 3 \otimes 3 = 10_S \oplus 8_M \oplus 8_M \oplus 1_A$$

Octet



Decuplet

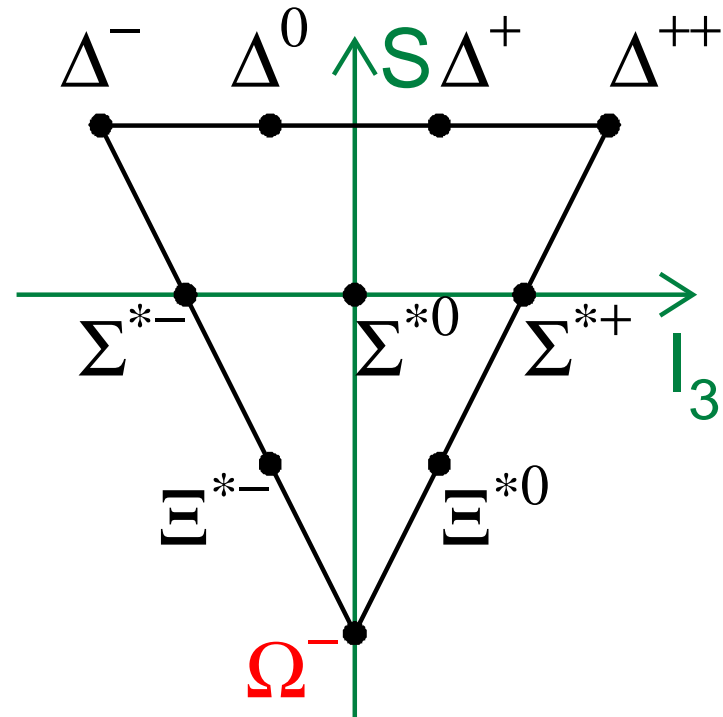


Table 2: Λ -hyperons used in the first fit of the data.

		J^P	Status	Mass	Width
singlet	$\Lambda(1405)$	$1/2^-$	****	$1405_{-1.0}^{+1.3}$	50.5 ± 2.0
$N(1535)$	$\Lambda(1670)$	$1/2^-$	****	$1660 - 1680$	$25 - 50$
$N(1650)$	$\Lambda(1800)$	$1/2^-$	***	$1720 - 1850$	$200 - 400$
singlet	$\Lambda(1520)$	$3/2^-$	****	1519.5 ± 1.0	15.6 ± 1.0
$N(1520)$	$\Lambda(1690)$	$3/2^-$	****	$1685 - 1695$	$50 - 70$
$N(1675)$	$\Lambda(1830)$	$5/2^-$	****	$1810 - 1830$	$60 - 110$
$N(2190)$	$\Lambda(2100)$	$7/2^-$	****	$2090 - 2110$	$100 - 250$
$N(1440)$	$\Lambda(1600)$	$1/2^+$	***	$1560 - 1700$	$50 - 250$
$N(1710)$	$\Lambda(1810)$	$1/2^+$	***	$1750 - 1850$	$50 - 250$
$N(1710)$	$\Lambda(1890)$	$3/2^+$	****	$1850 - 1910$	$60 - 200$
$N(1680)$	$\Lambda(1820)$	$5/2^+$	****	$1815 - 1825$	$70 - 90$
$N(2060)$	$\Lambda(2110)$	$5/2^+$	***	$2090 - 2140$	$150 - 250$

Table 3: Σ -Hyperons used in the first fit of the data.

		J^P	Status	Mass	Width
$N(1440)$	$\Sigma(1660)$	$1/2^+$	***	1630 – 1690	36.0 ± 0.7
$\Delta(1230)$	$\Sigma(1385)$	$3/2^+$	****	1382.80 ± 0.35	40 – 200
$N(1680), \Delta(1905)$	$\Sigma(1915)$	$5/2^+$	****	1900 – 1935	80 – 160
$N(1990), \Delta(1950)$	$\Sigma(2030)$	$7/2^+$	****	2025 – 2040	150 – 200
$N(1520)$	$\Sigma(1670)$	$3/2^-$	****	1665 – 1685	40 – 80
$N(1535), \Delta(1620), N(1650)$	$\Sigma(1750)$	$1/2^-$	***	1730 – 1800	60 – 160
$N(1675)$	$\Sigma(1775)$	$5/2^-$	****	1770 – 1780	105 – 135
$N(1700), \Delta(1700)$	$\Sigma(1940)$	$3/2^-$	***	1900 – 1950	150 – 300

Many Σ states are missing.

Kaon beam motivation

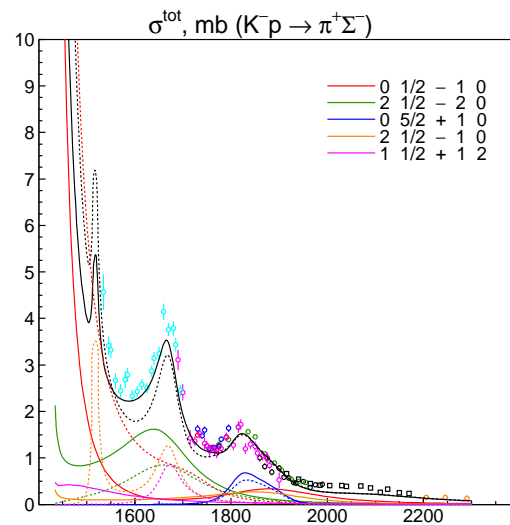
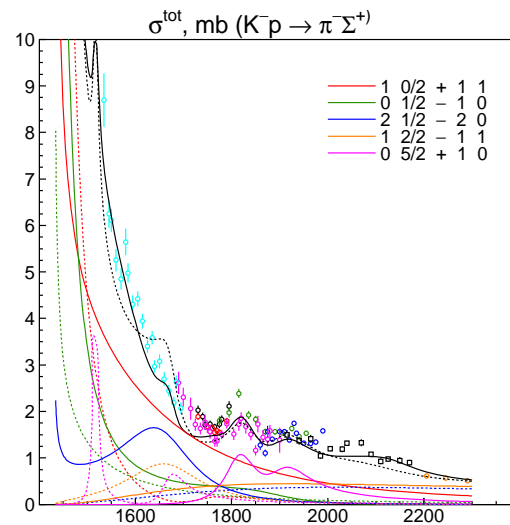
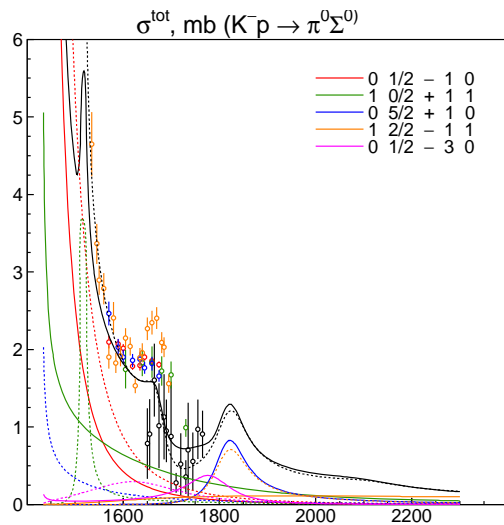
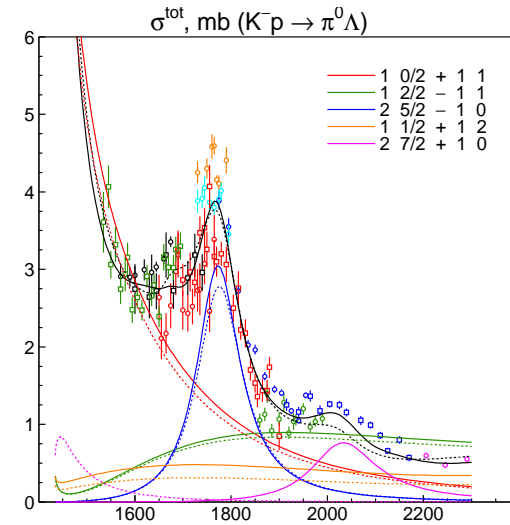
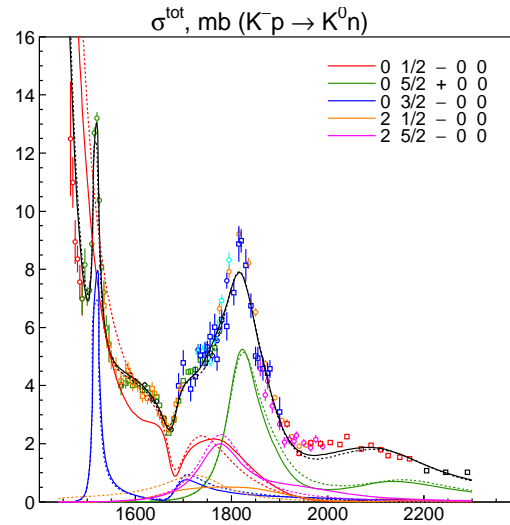
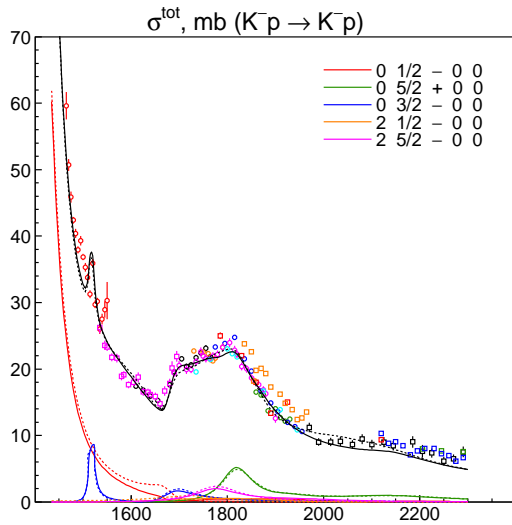
There is a hope to observe the baryon multiplets and therefore to confirm the states observed in the Nucleon and Delta sector.

Table 4: List of reactions used in the partial wave analysis.

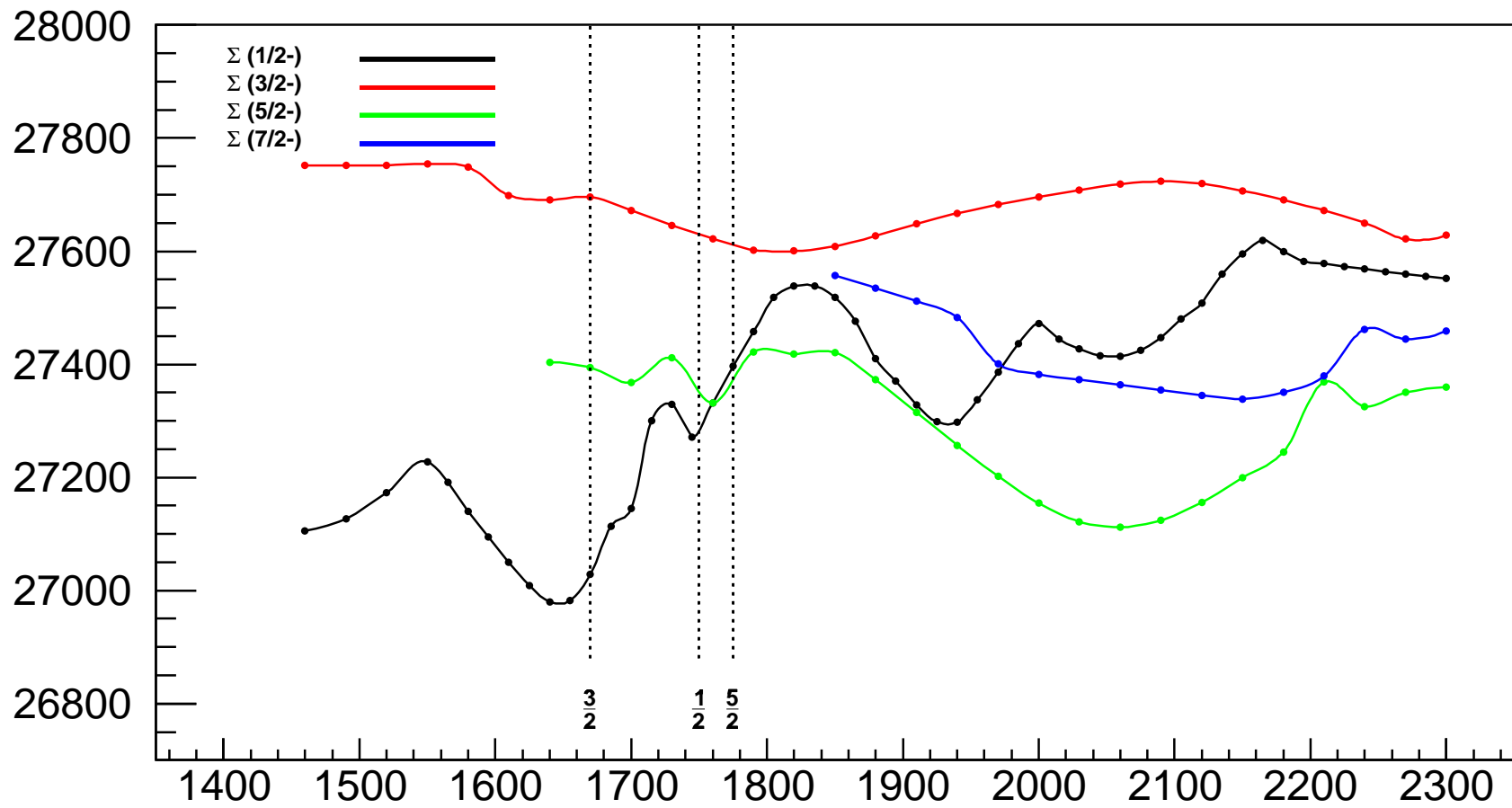
$K^- p \rightarrow K^0 n$	$K^- p \rightarrow K^- p$	$K^- p \rightarrow \omega \Lambda$
$K^- p \rightarrow \pi^0 \Lambda$	$K^- p \rightarrow \eta \Lambda$	$K^- p \rightarrow \pi^+ \Sigma^-$
$K^- p \rightarrow \pi^0 \Sigma^0$	$K^- p \rightarrow \pi^- \Sigma^+$	$K^- p \rightarrow \pi^0 \pi^0 \Lambda$
$K^- p \rightarrow K^+ \Xi^-$	$K^- p \rightarrow K^0 \Xi^0$	$K^- p \rightarrow \pi^0 \pi^0 \Sigma^0$

W range is 1.57 – 1.68

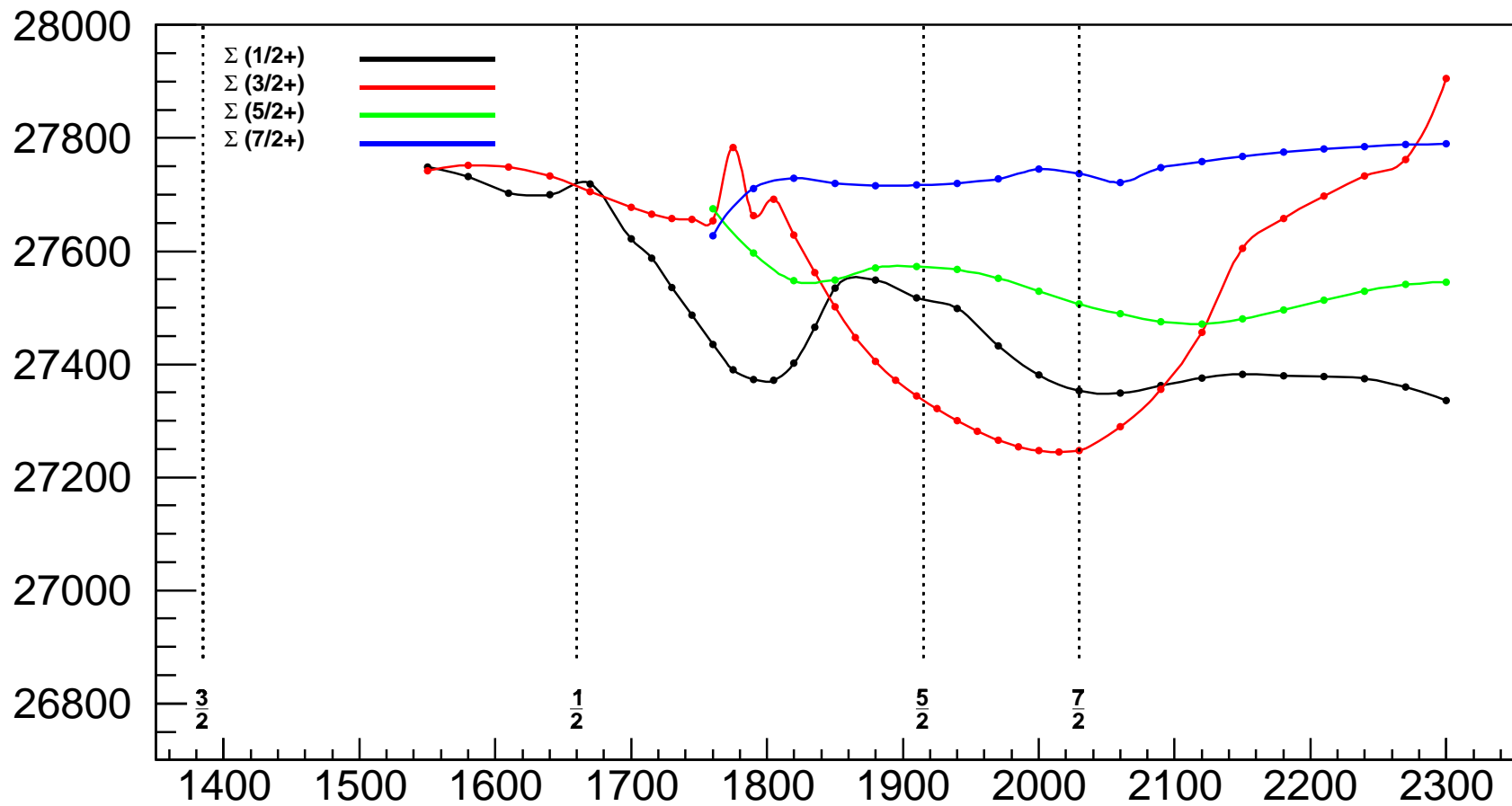
Analysis of the Kp collision reactions (Preliminary) (M. Matveev)



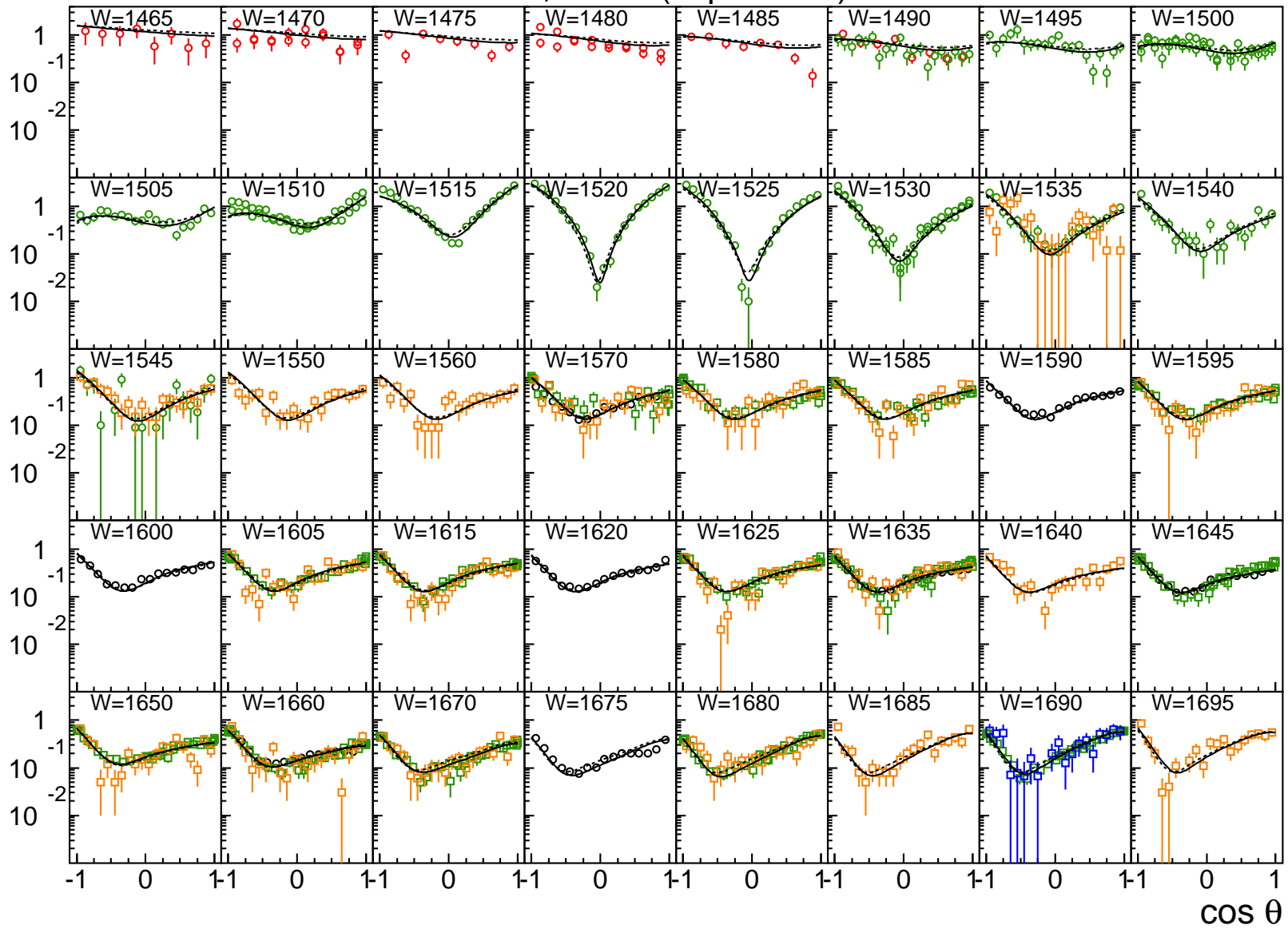
$\Sigma (-)$



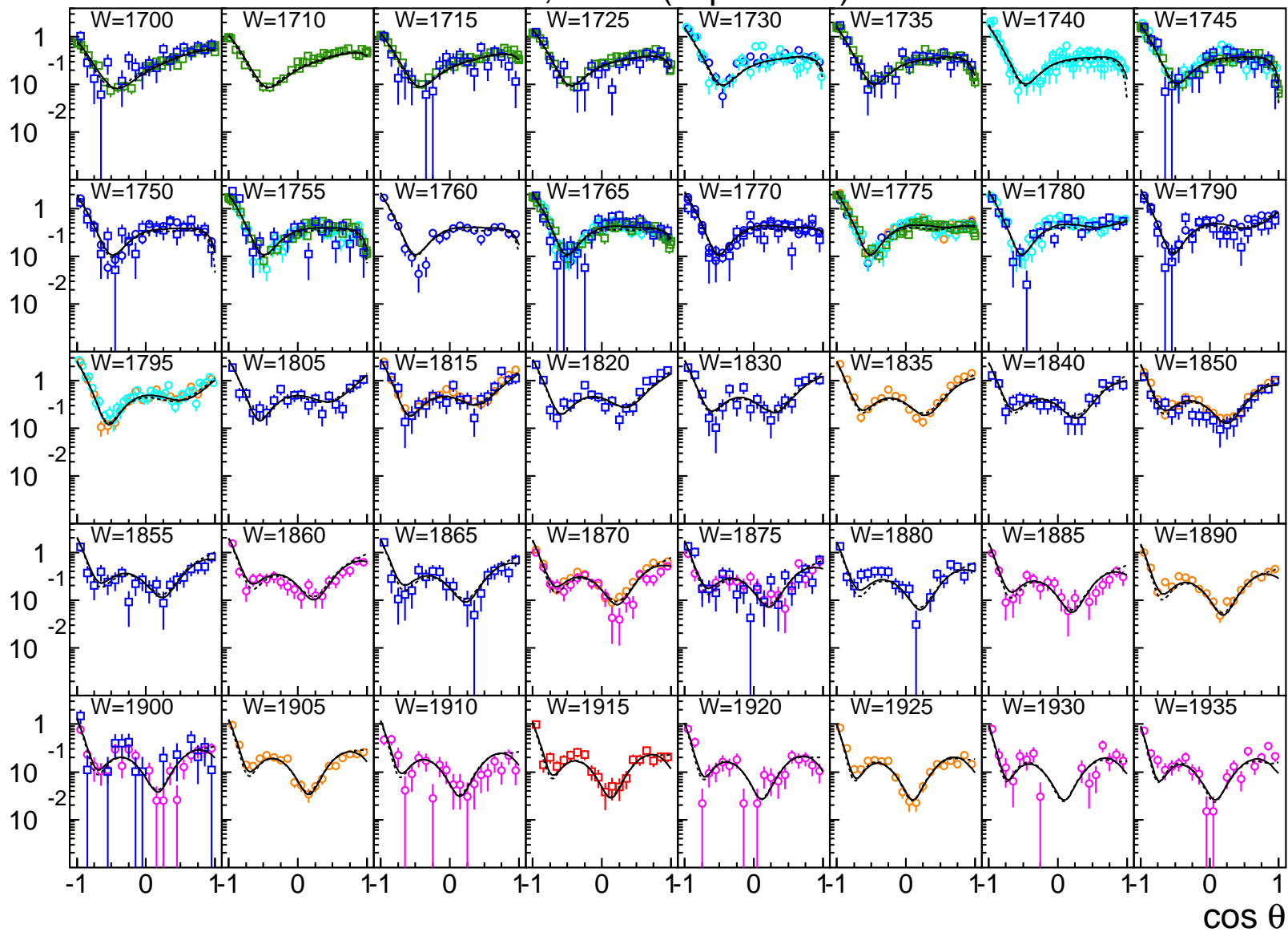
$\Sigma (+)$



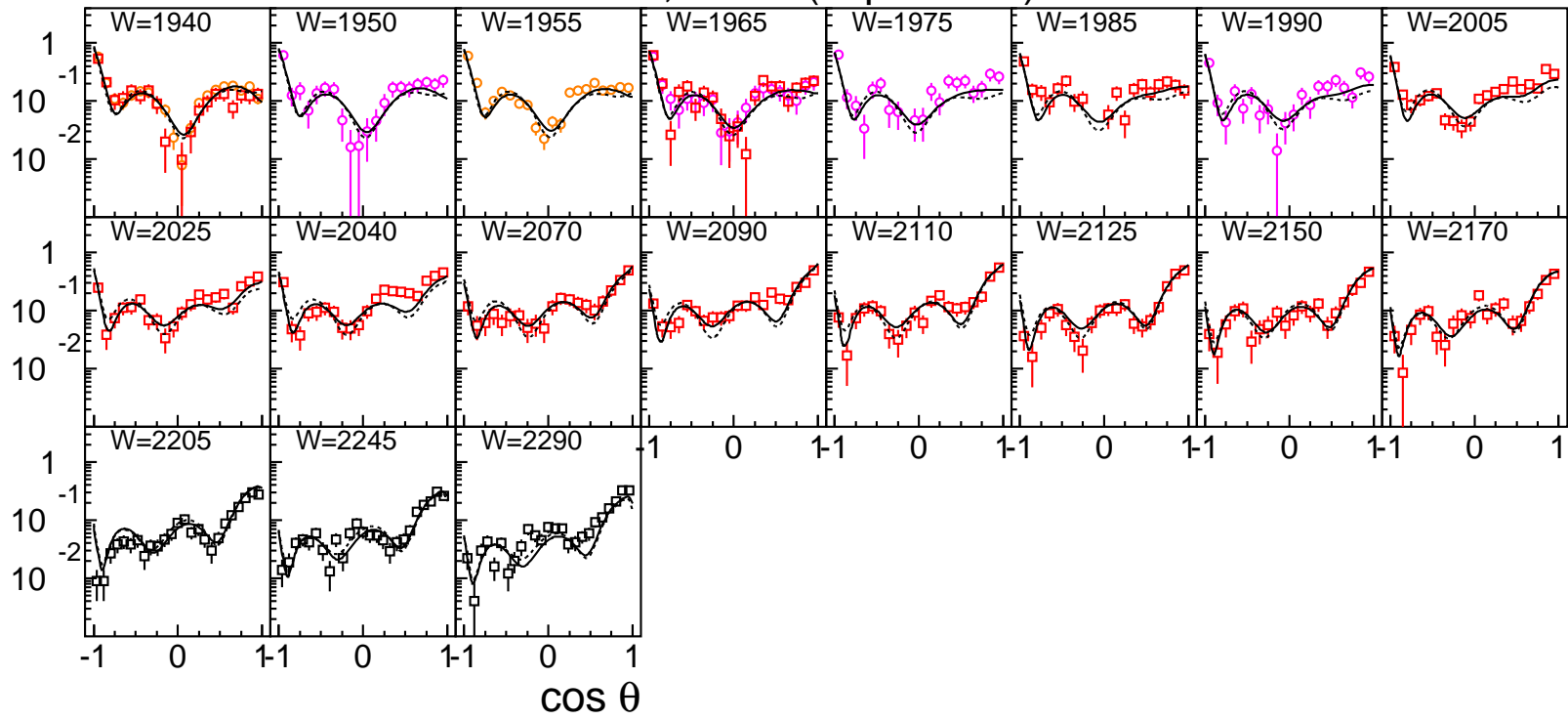
$d\sigma/d\Omega$, mb/sr ($K^-p \rightarrow K^0n$)



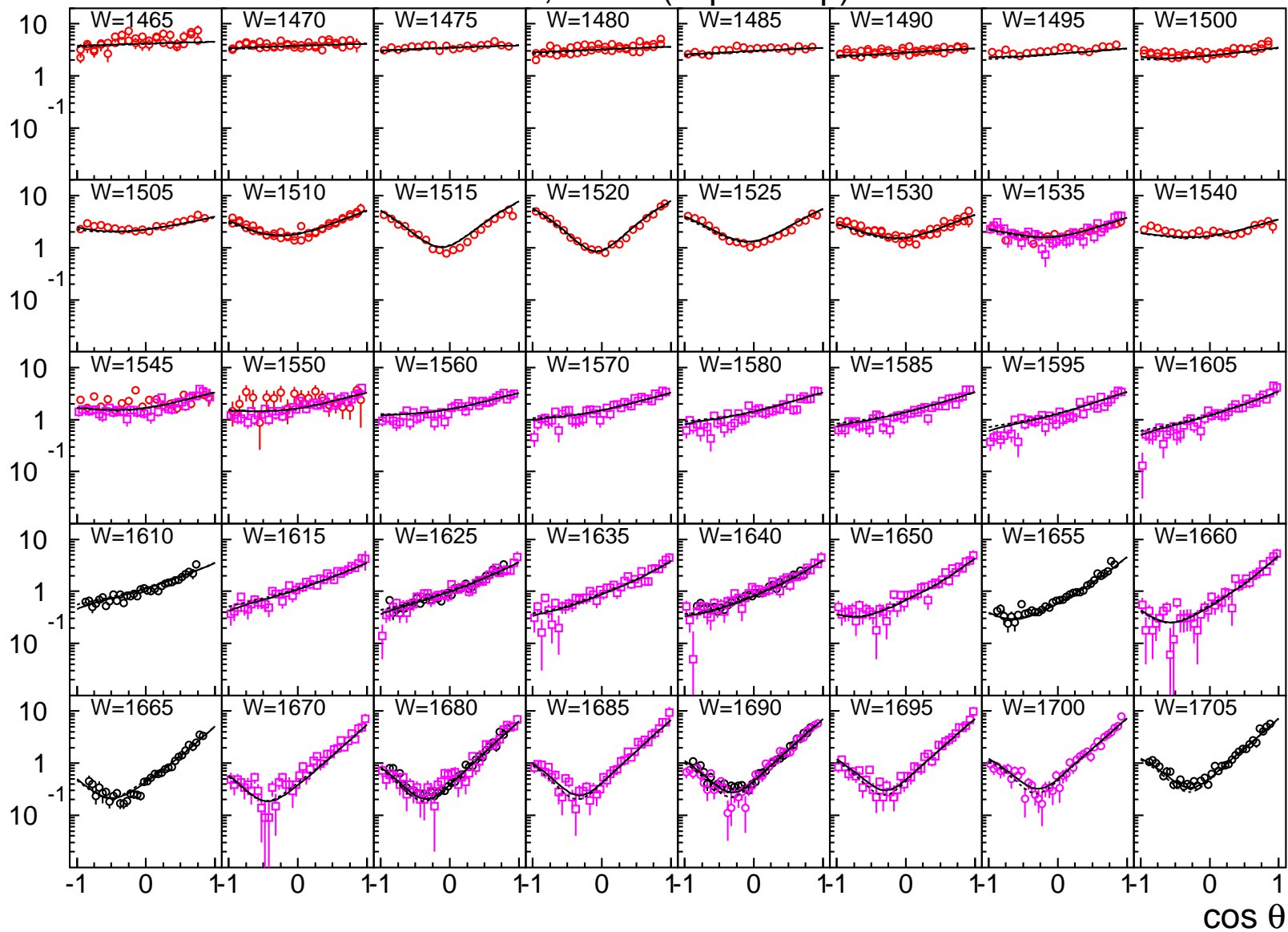
$d\sigma/d\Omega$, mb/sr ($K^-p \rightarrow K^0n$)



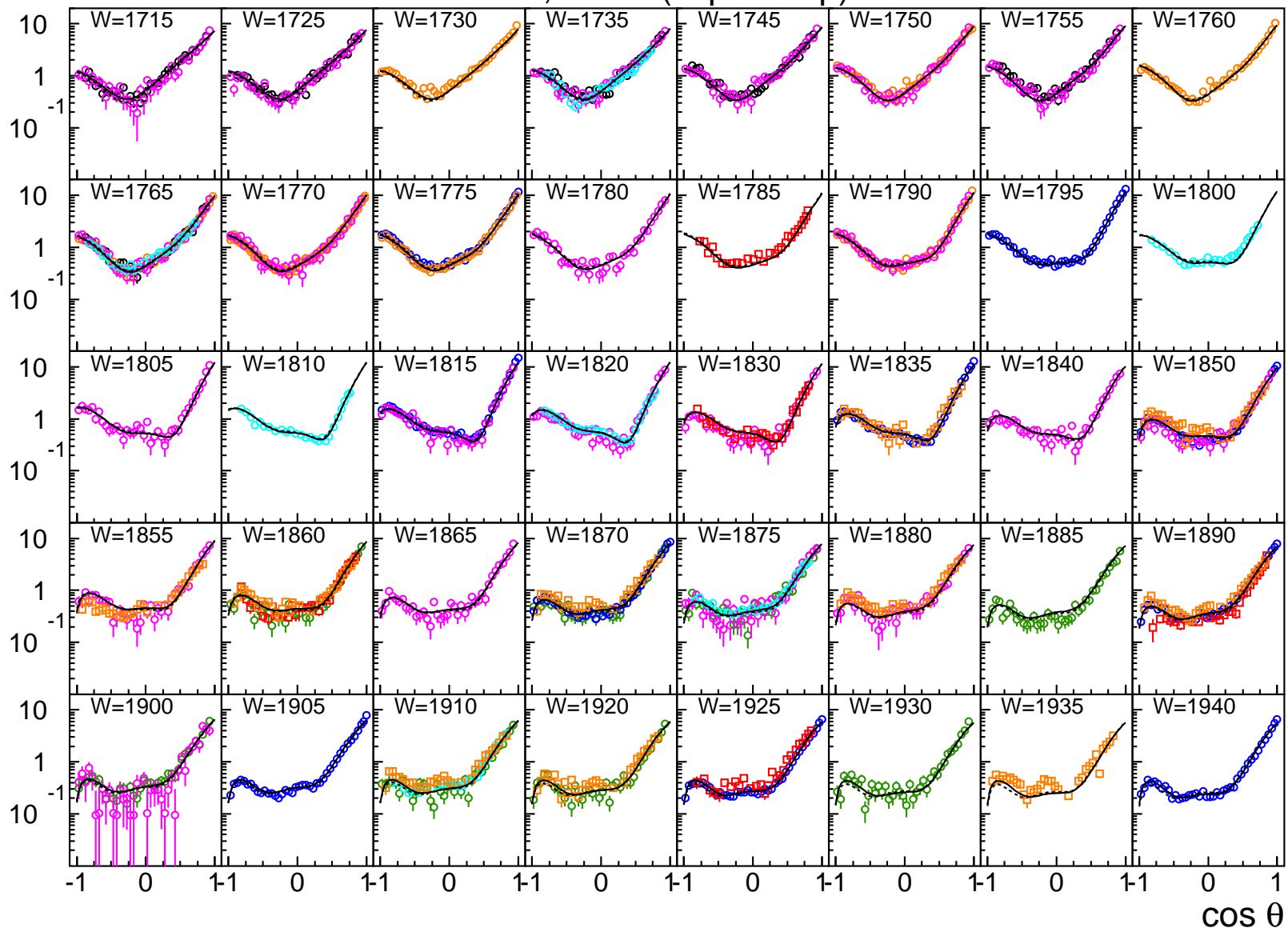
$d\sigma/d\Omega, \text{mb/sr} (K^-p \rightarrow K^0n)$



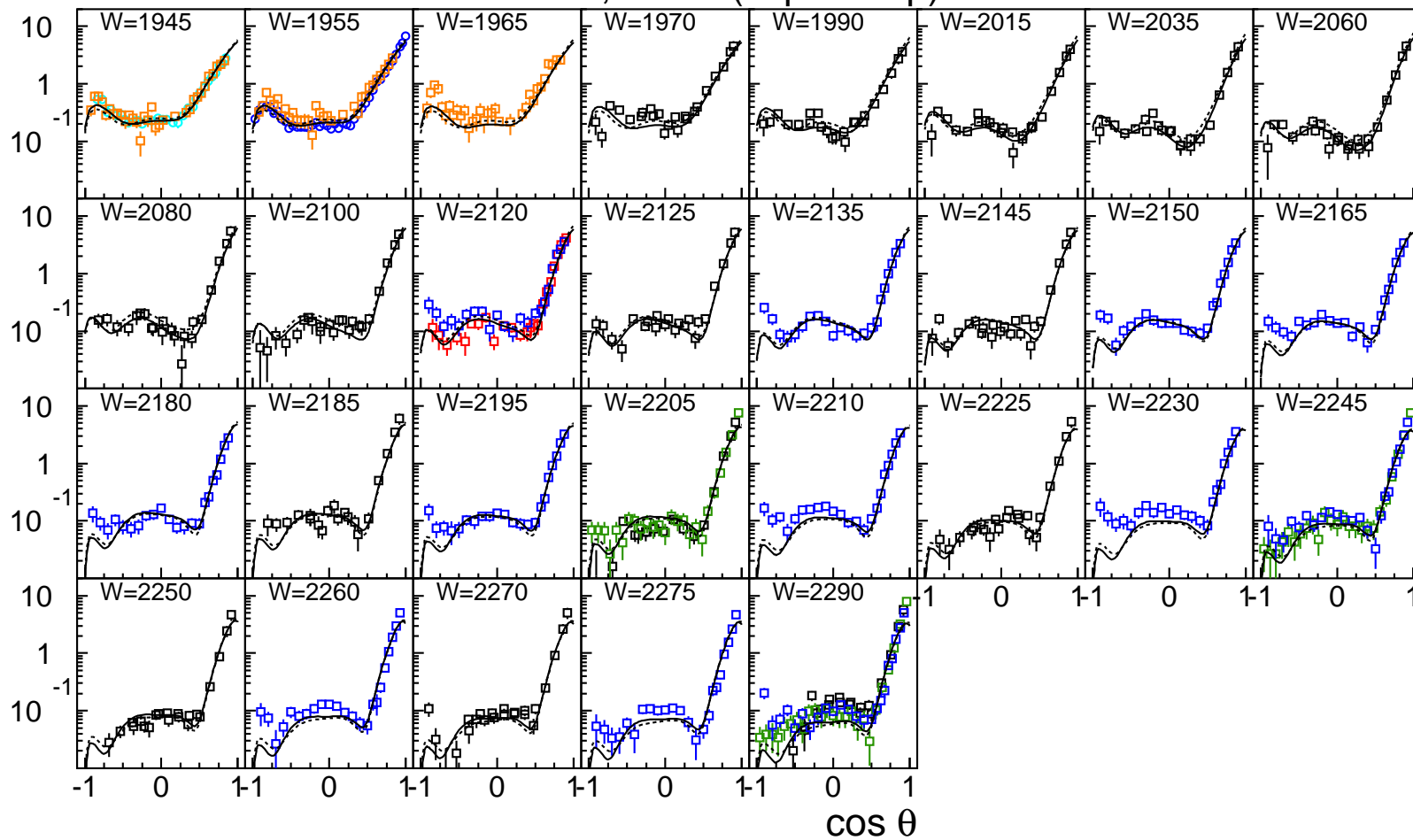
$d\sigma/d\Omega$, mb/sr ($K^- p \rightarrow K^- p$)



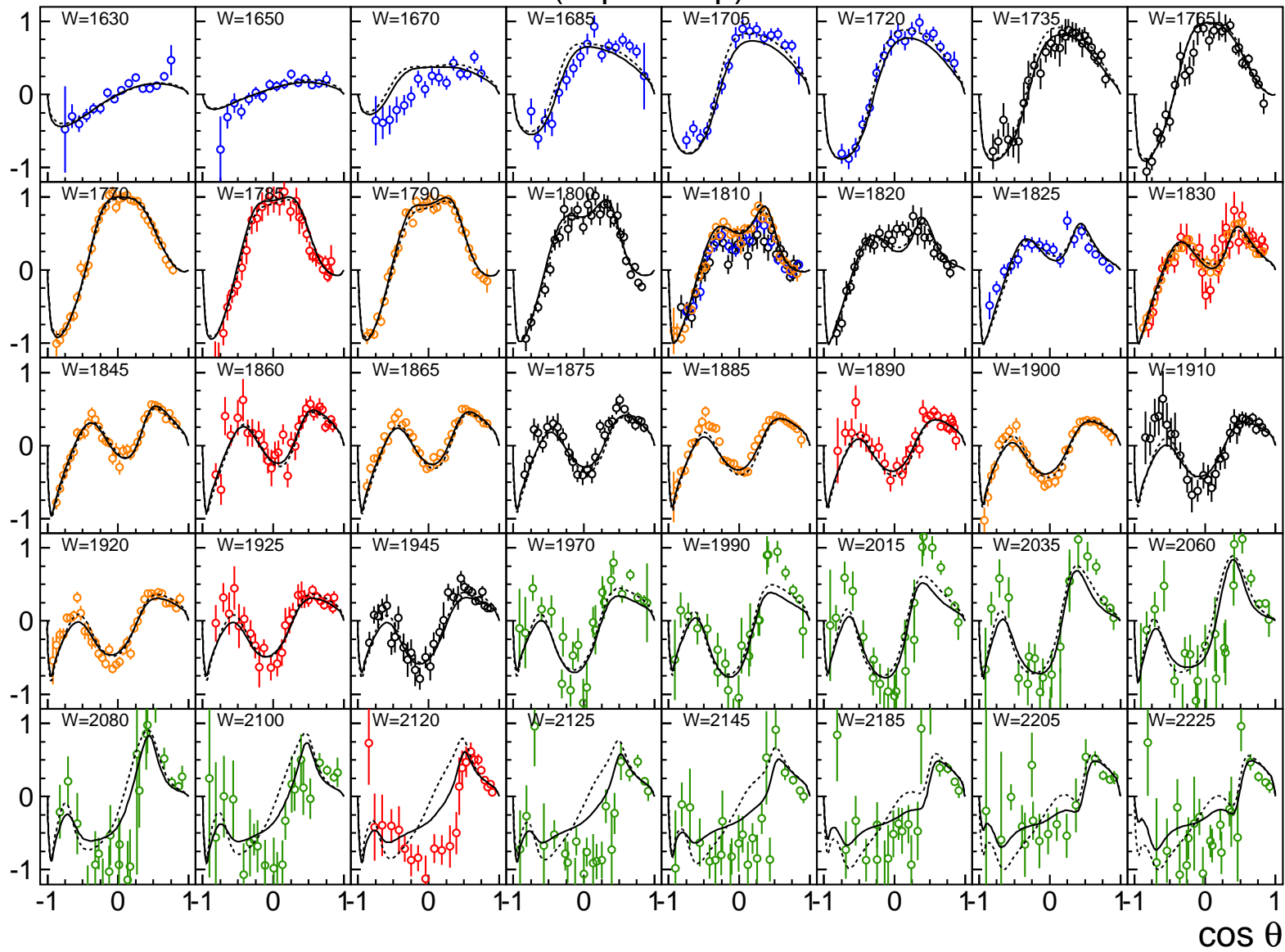
$d\sigma/d\Omega$, mb/sr ($K^- p \rightarrow K^- p$)



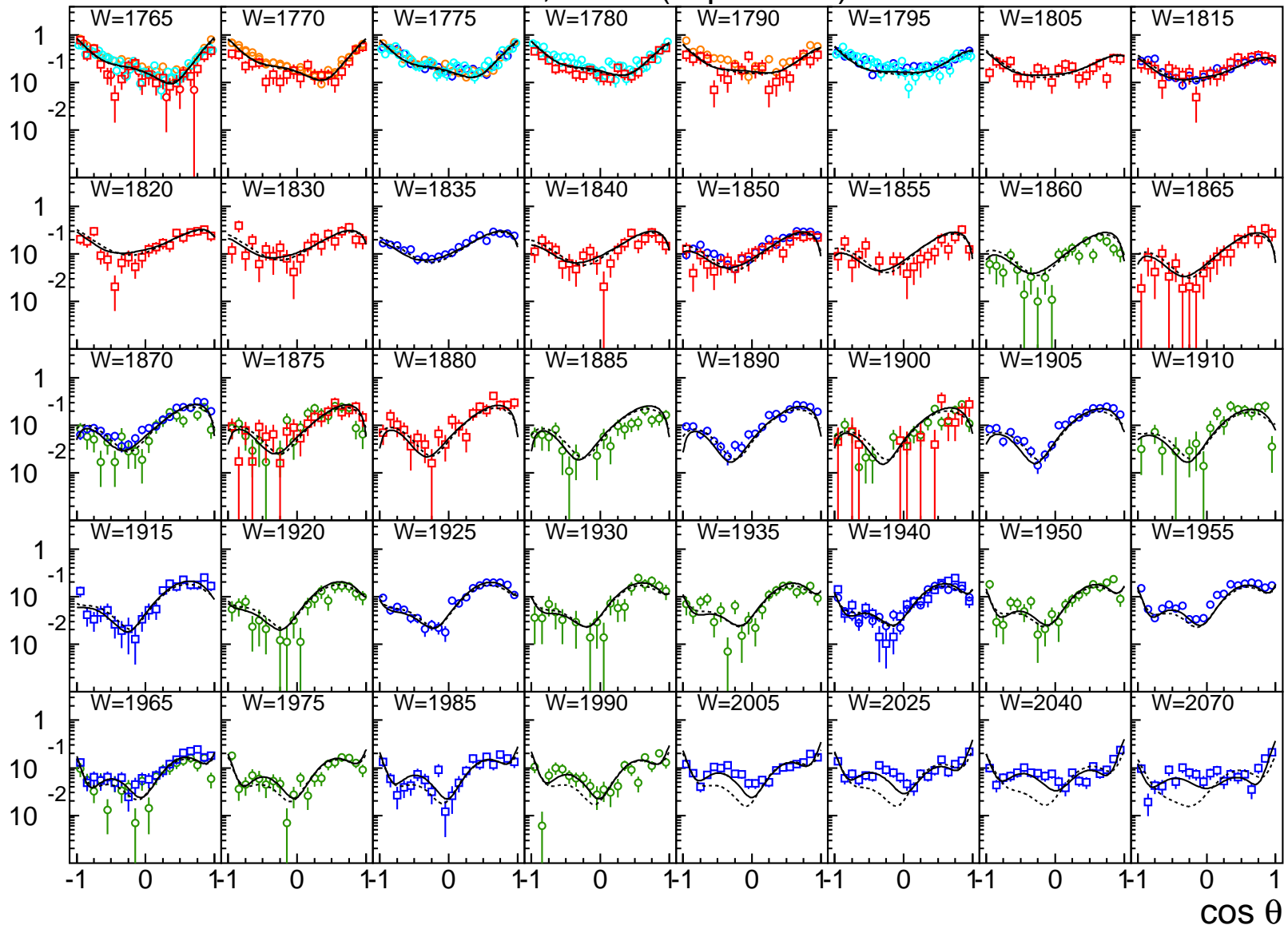
$d\sigma/d\Omega$, mb/sr ($K^- p \rightarrow K^- p$)

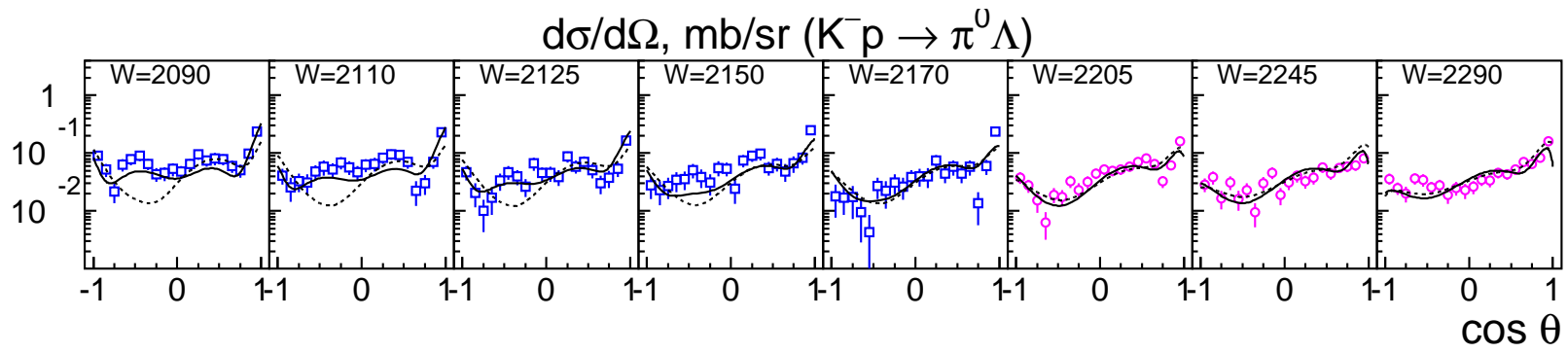


$P(K^-p \rightarrow K^-p)$

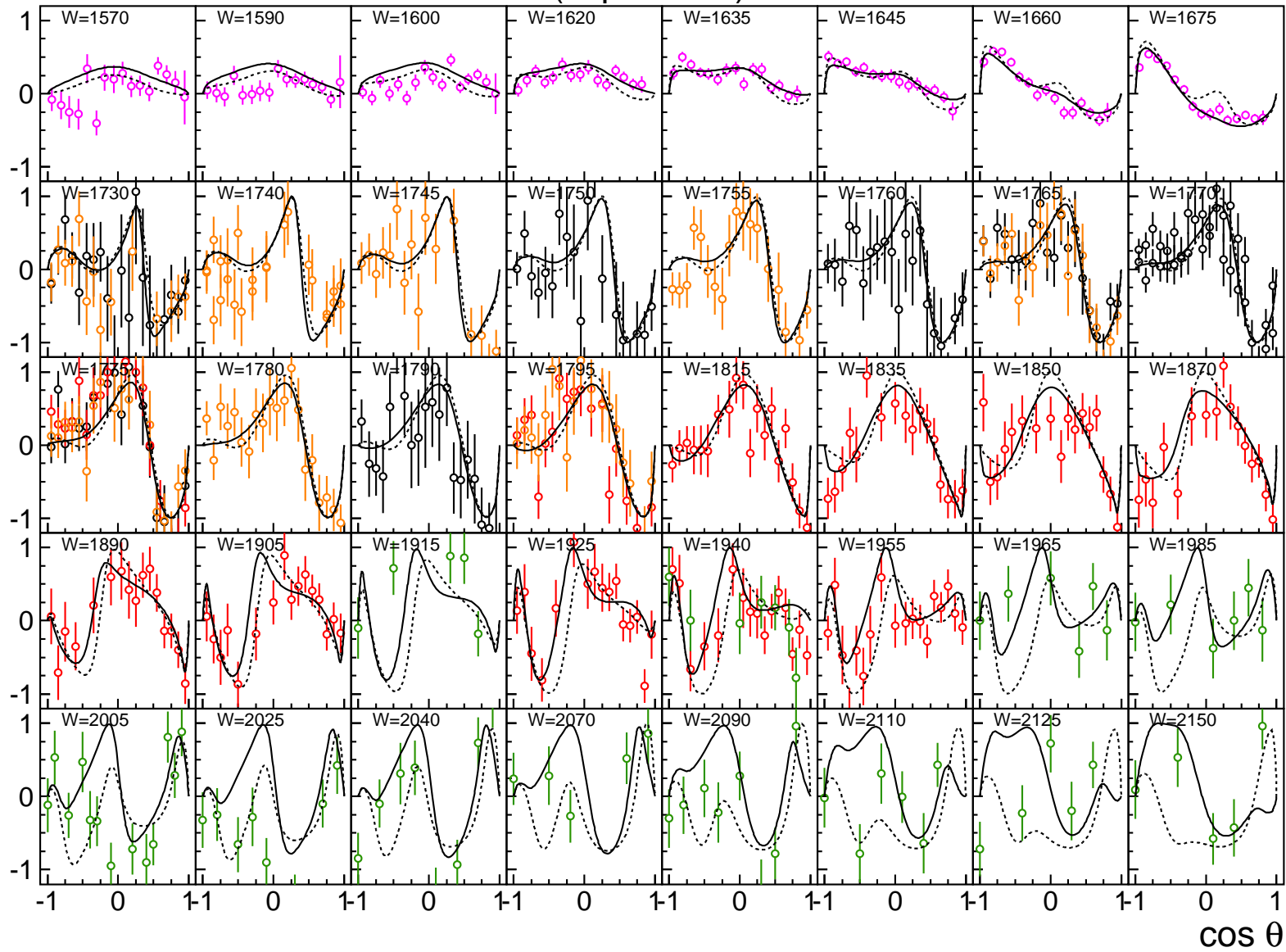


$d\sigma/d\Omega, \text{mb/sr} (K^- p \rightarrow \pi^0 \Lambda)$

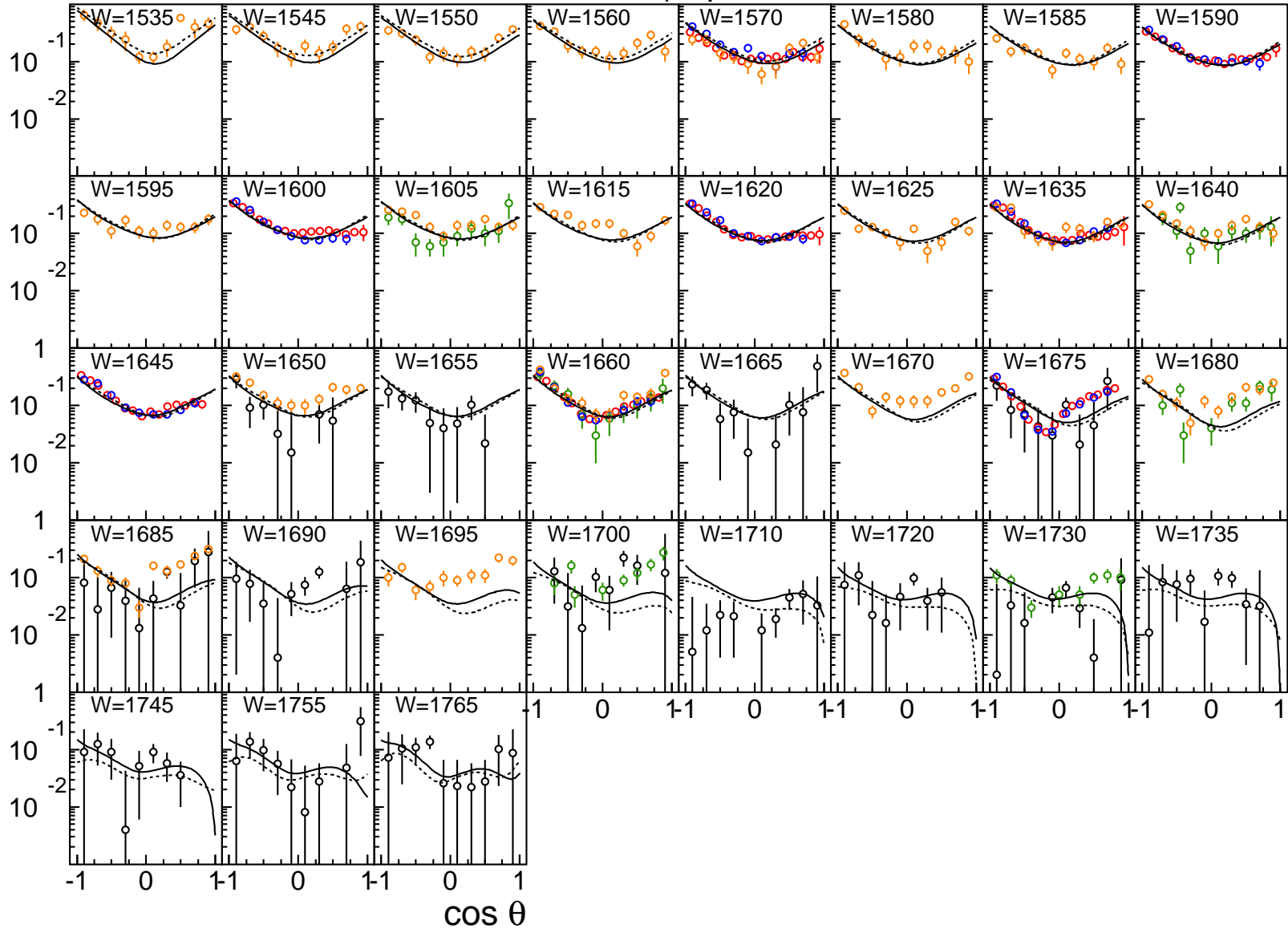


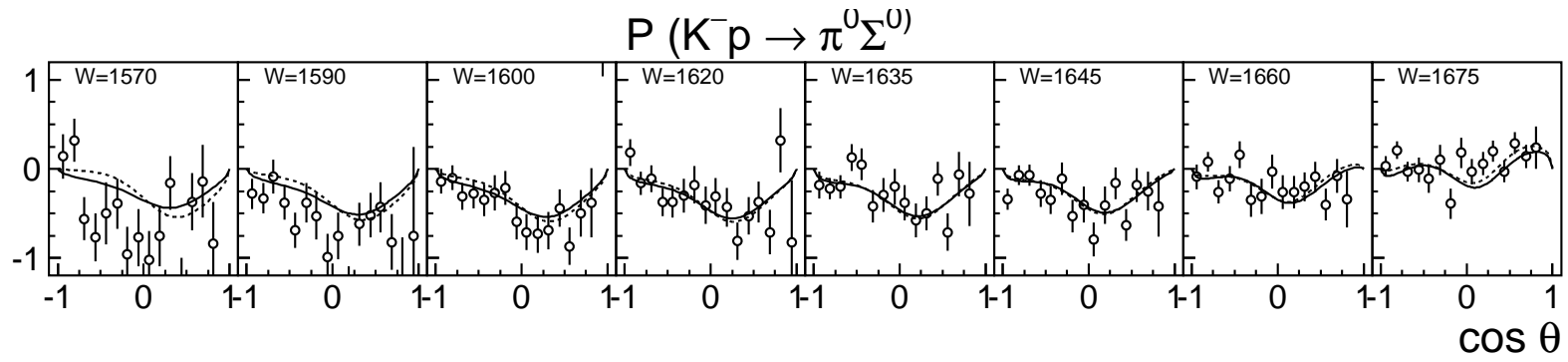


$P(K^- p \rightarrow \pi^0 \Lambda)$

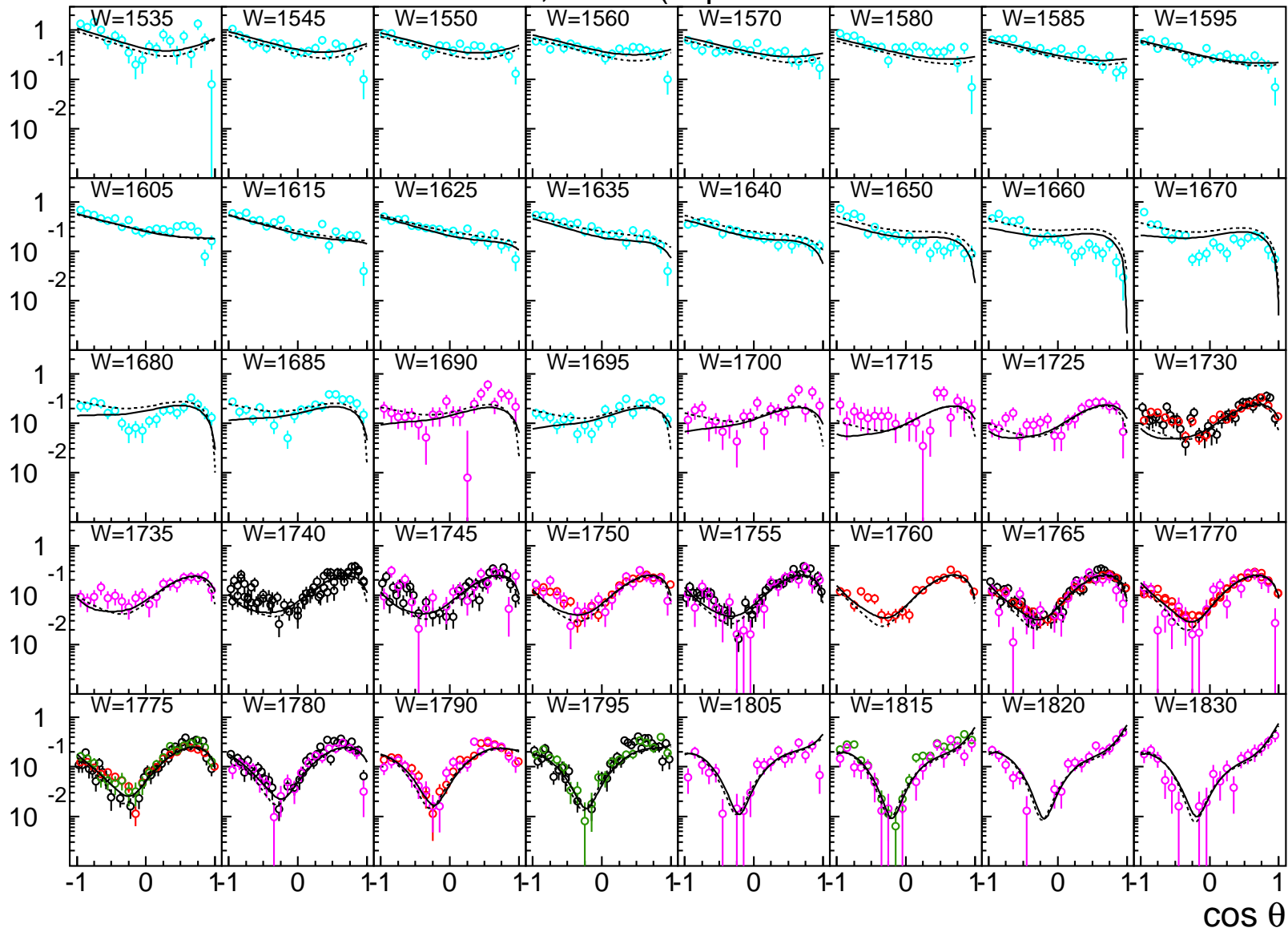


$d\sigma/d\Omega$, mb/sr ($K^- p \rightarrow \pi^0 \Sigma^0$)

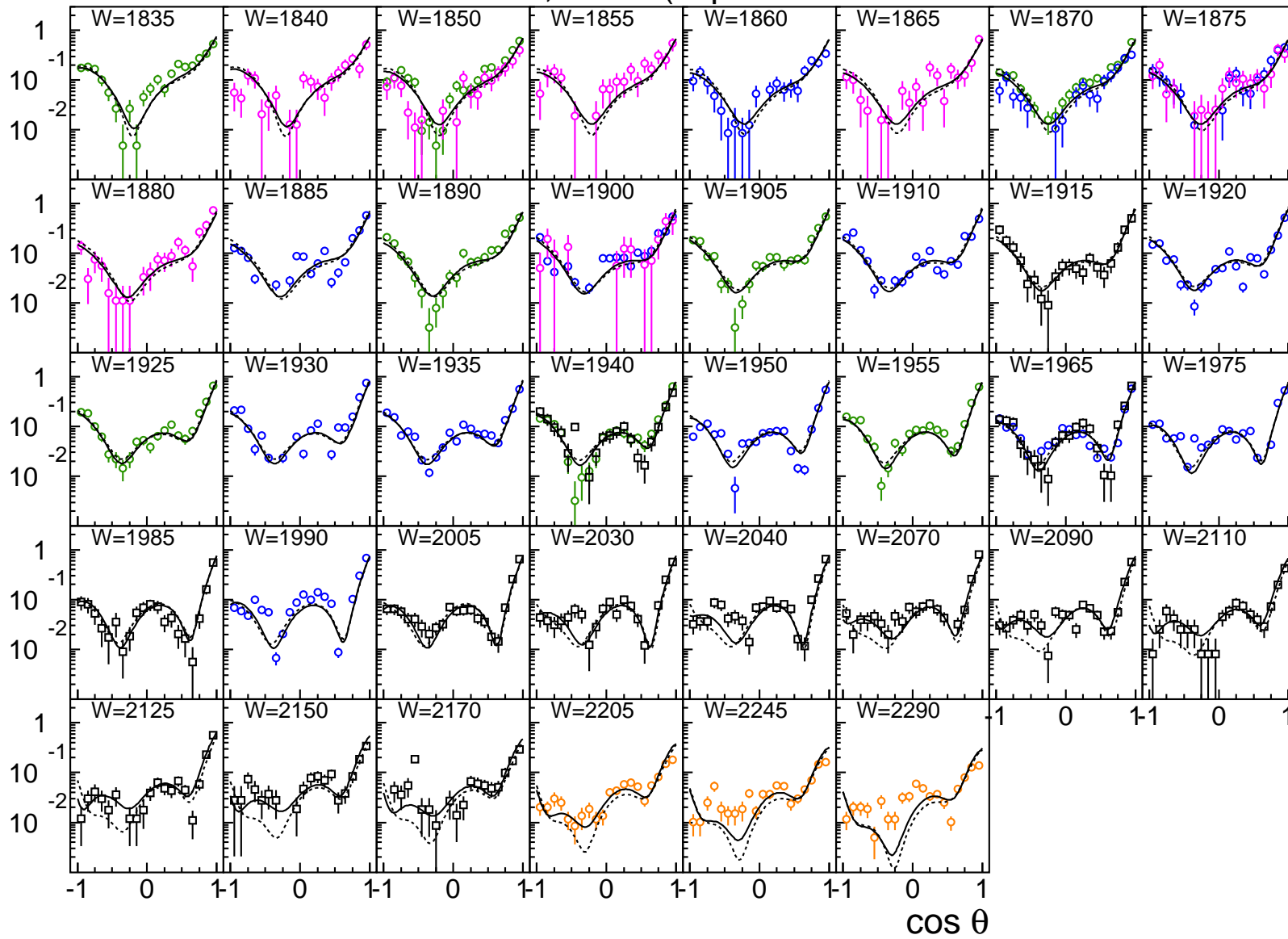




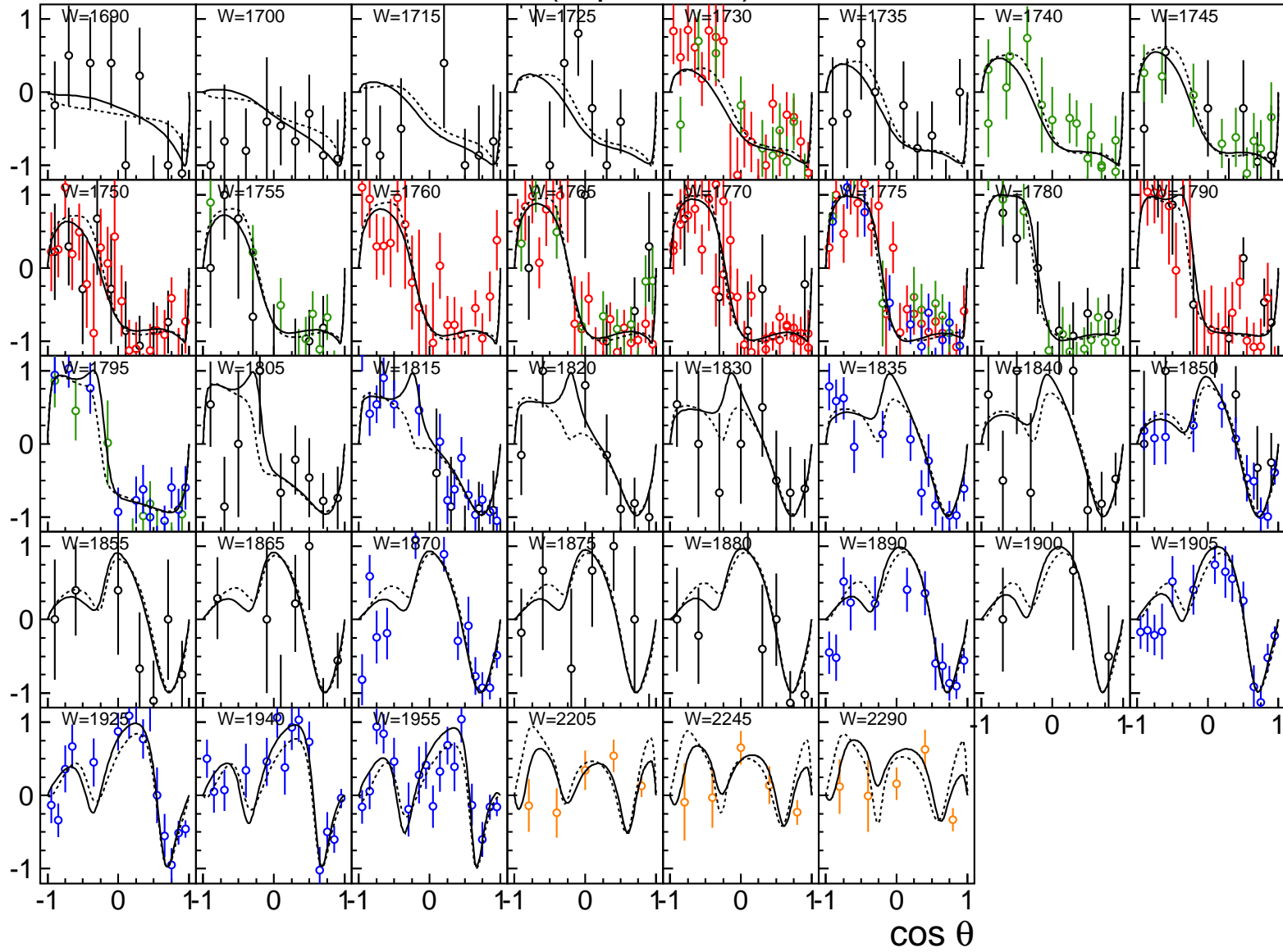
$d\sigma/d\Omega, \text{ mb/sr } (K^- p \rightarrow \pi^- \Sigma^+)$



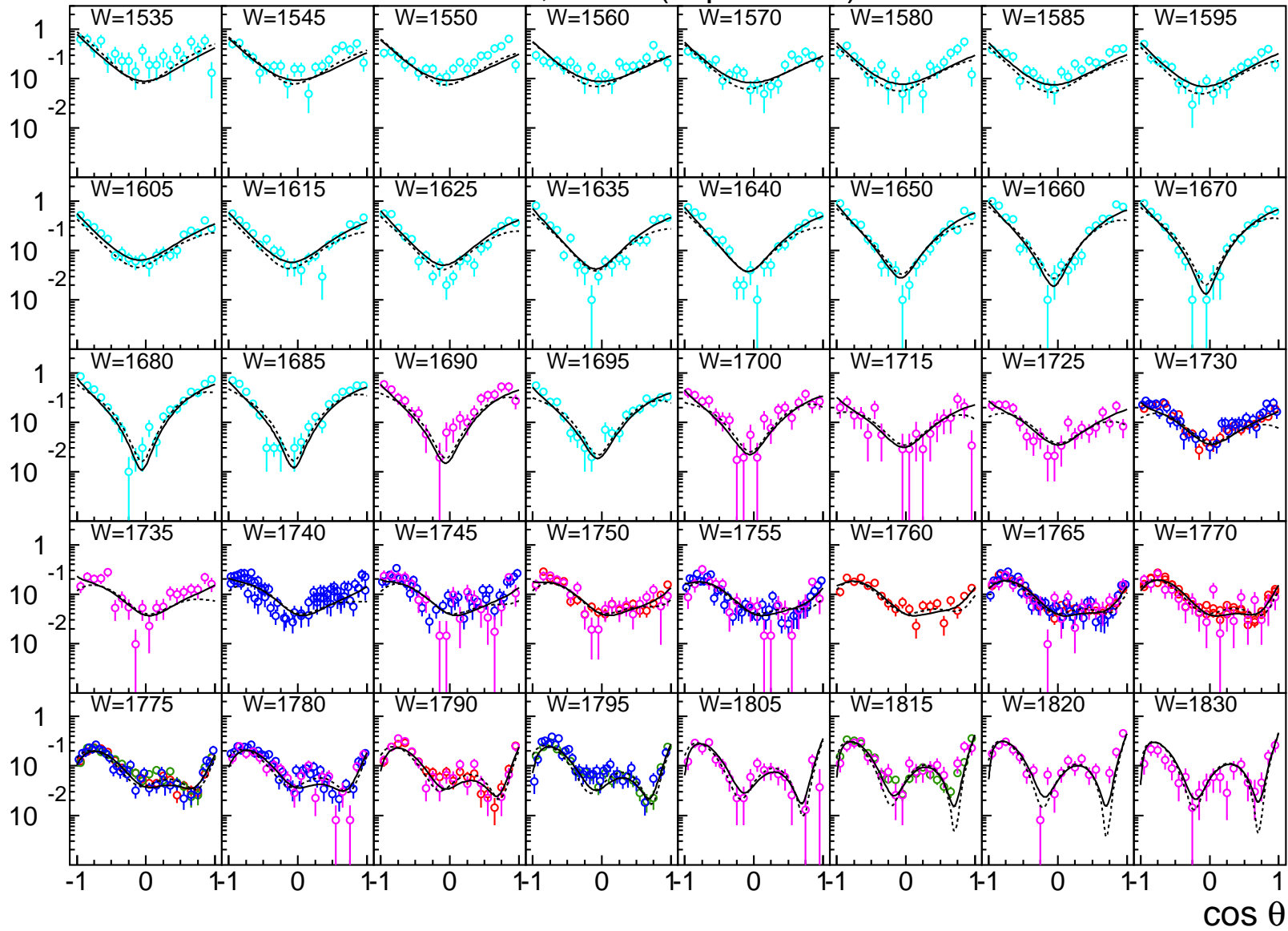
$d\sigma/d\Omega, \text{ mb/sr } (K^- p \rightarrow \pi^- \Sigma^+)$



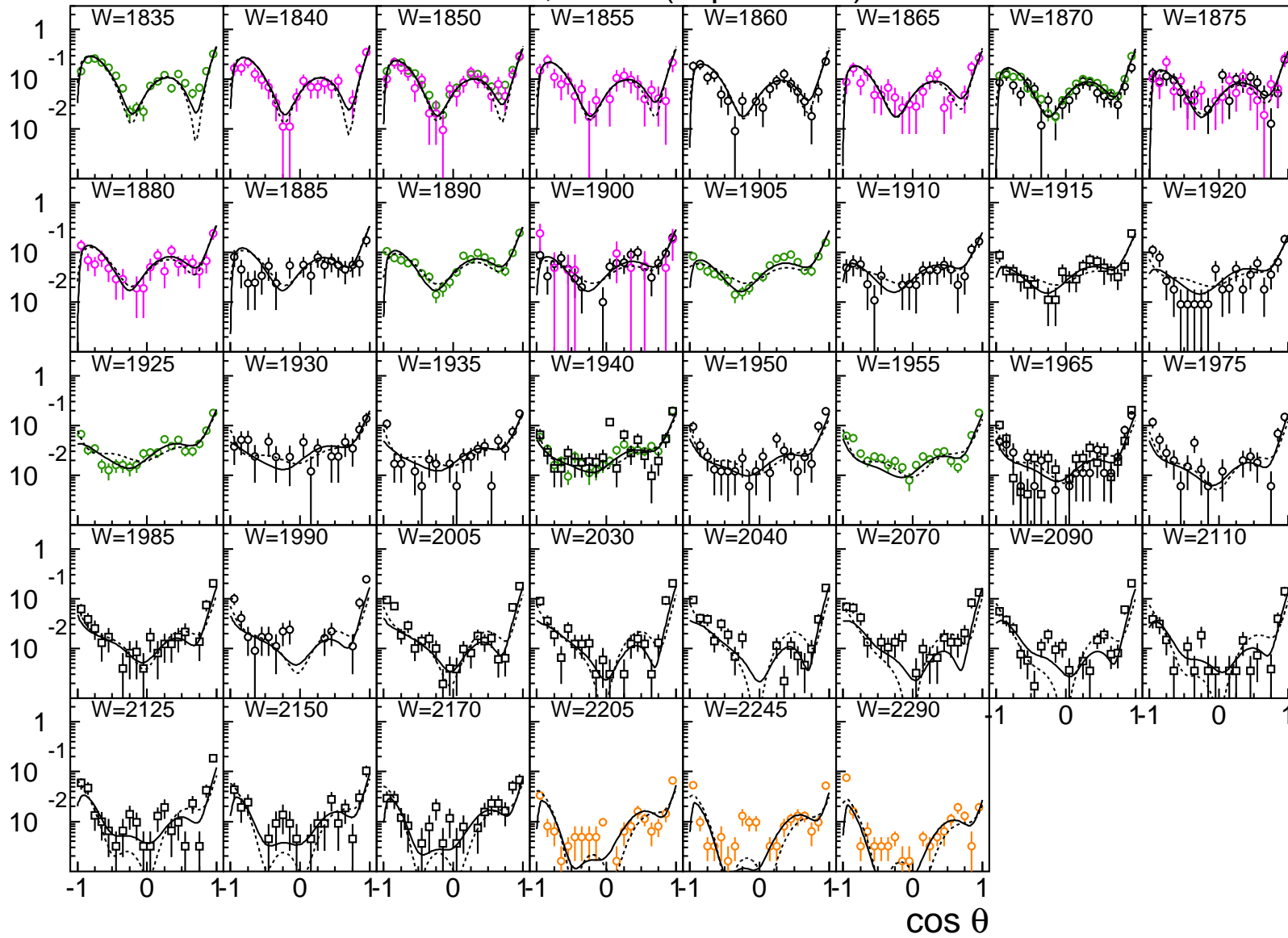
$P(K^- p \rightarrow \pi^- \Sigma^+)$



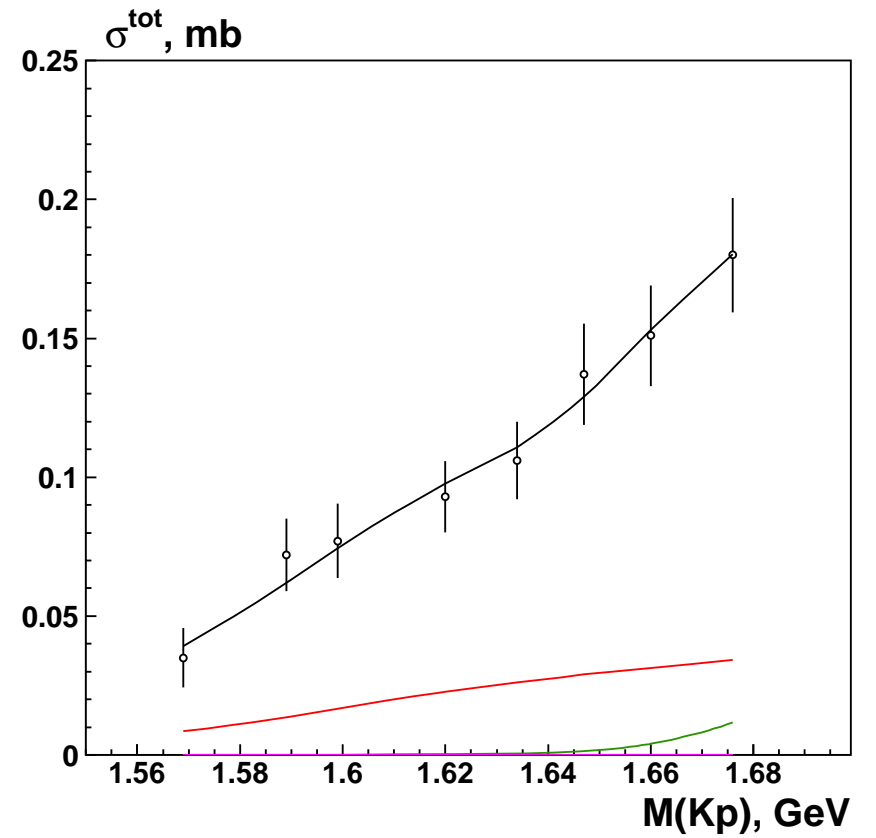
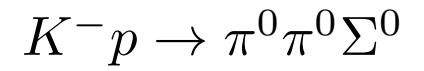
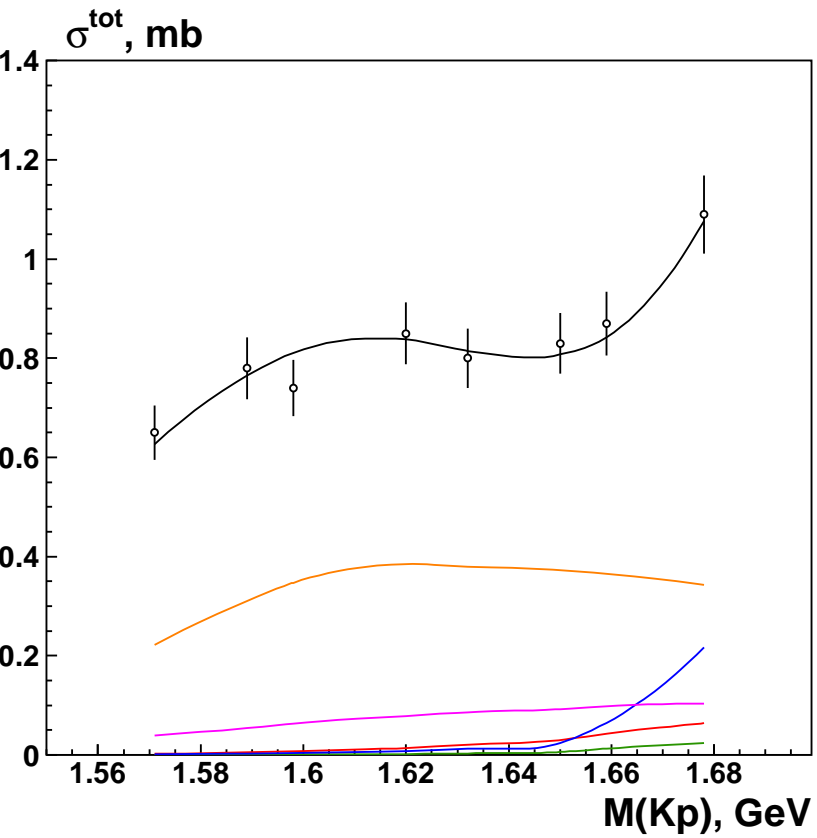
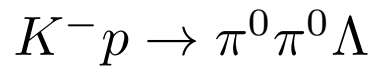
$d\sigma/d\Omega, \text{ mb/sr } (K^- p \rightarrow \pi^+ \Sigma^-)$



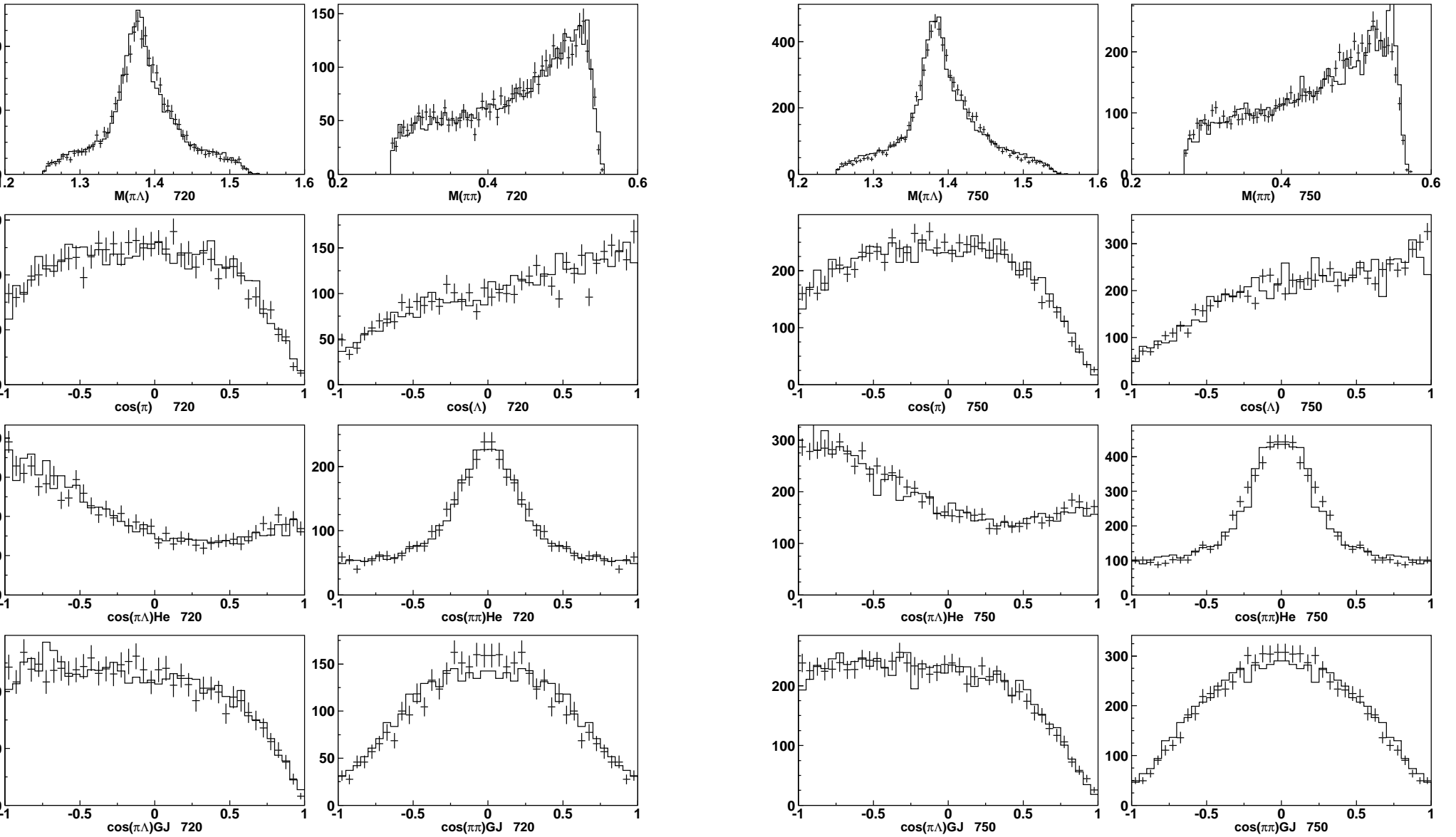
$d\sigma/d\Omega, \text{ mb/sr } (K^- p \rightarrow \pi^+ \Sigma^-)$



		ANL-Osaca	Bn-Ga	Model A	Model B	Bn-Ga
$K^- p \rightarrow K^- p$	$d\sigma/d\Omega$	3962	5495	3.07	2.98	2.28
	P	510	859	2.04	2.08	1.79
$K^- p \rightarrow \bar{K}^0 n$	$d\sigma/d\Omega$	2950	3445	2.67	2.75	1.62
$K^- p \rightarrow \pi^- \Sigma^+$	$d\sigma/d\Omega$	1792	2095	3.37	3.49	3.17
	P	418	578	1.30	1.28	2.06
$K^- p \rightarrow \pi^0 \Sigma^0$	$d\sigma/d\Omega$	580	581	3.68	3.50	3.57
	P	196	124	6.39	5.80	1.51
$K^- p \rightarrow \pi^+ \Sigma^-$	$d\sigma/d\Omega$	1786	2082	2.56	2.18	1.80
$K^- p \rightarrow \pi^0 \Lambda$	$d\sigma/d\Omega$	2178	2478	2.59	3.71	1.82
	P	693	732	1.41	1.73	1.73
$K^- p \rightarrow \eta \Lambda$	$d\sigma/d\Omega$	160	160	2.69	2.03	1.52
	P	18	—	0.94	3.83	—
$K^- p \rightarrow K^0 \Xi^0$	$d\sigma/d\Omega$	33	67	1.24	1.61	1.20
$K^- p \rightarrow K^+ \Xi^-$	$d\sigma/d\Omega$	92	193	2.05	1.74	1.38
$K^- p \rightarrow \Lambda \omega$	$d\sigma/d\Omega$	—	300	—	—	1.08



$K^- p \rightarrow \pi^0 \pi^0 \Lambda$ (beam momenta 720 and 750 MeV/c)



$K^- p \rightarrow \pi^0 \pi^0 \Sigma^0$ (beam momenta 720 and 750 MeV/c)

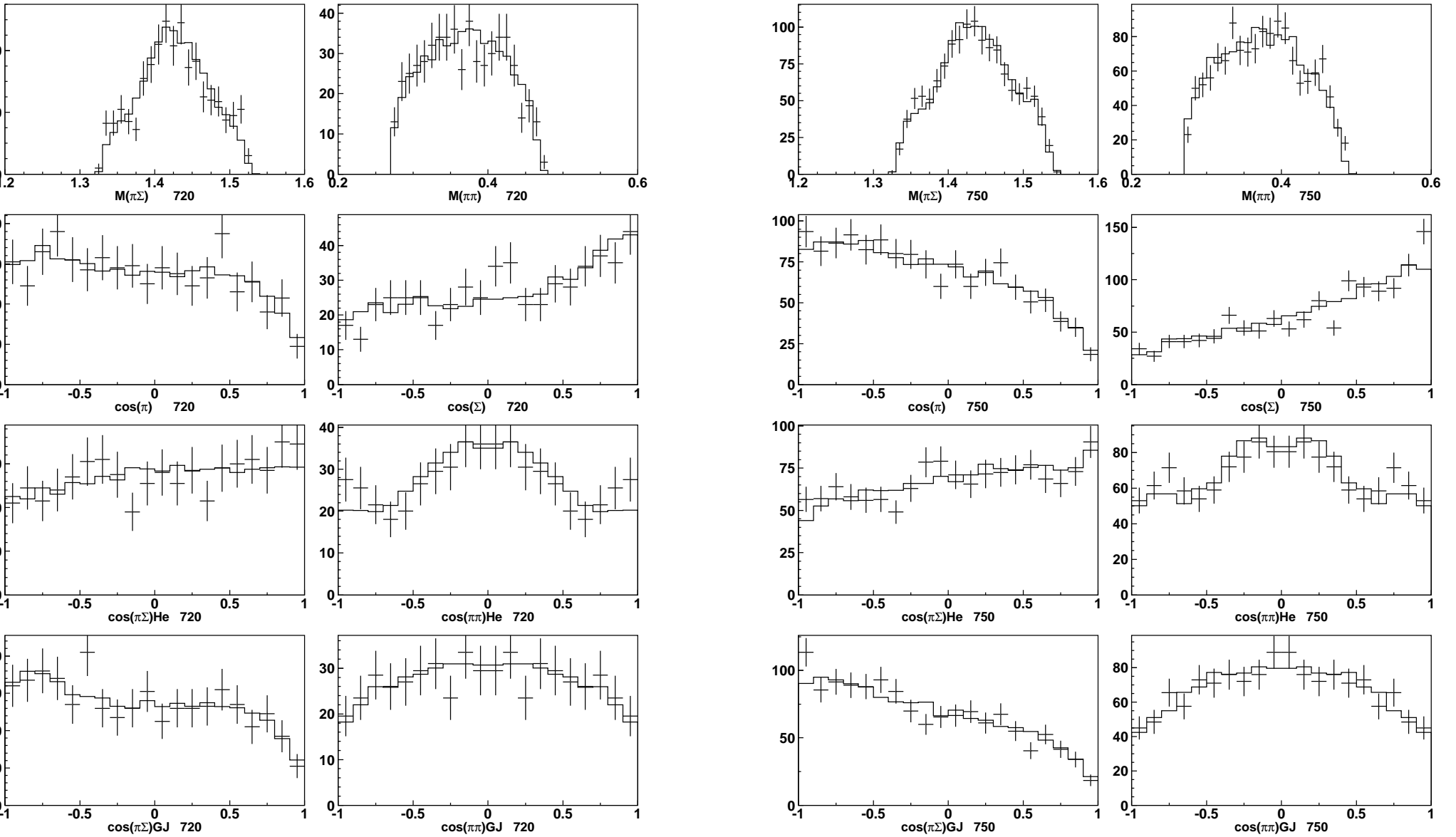


Table 5: Σ -Hyperons used in the first fit to the data.

	J^P	Status	Mass	Width
$\Sigma(1660)$	$1/2^+$	***	1630 – 1690	36.0 ± 0.7
$\Sigma(1385)$	$3/2^+$	****	1382.80 ± 0.35	40 – 200
$\Sigma(1915)$	$5/2^+$	****	1900 – 1935	80 – 160
$\Sigma(2030)$	$7/2^+$	****	2025 – 2040	150 – 200
$\Sigma(1670)$	$3/2^-$	****	1665 – 1685	40 – 80
$\Sigma(1750)$	$1/2^-$	***	1730 – 1800	60 – 160
$\Sigma(1775)$	$5/2^-$	****	1770 – 1780	105 – 135
$\Sigma(1940)$	$3/2^-$	***	1900 – 1950	150 – 300
$\Sigma(1665)$	$1/2^-$		1670 ± 15	210 ± 20
$\Sigma(2150)$	$1/2^-$		2160 ± 20	220 ± 25
$\Sigma(2250)$	$5/2^-$		2250 ± 30	330 ± 40

SUMMARY

- The energy independent analysis of the $\gamma p \rightarrow K\Lambda$ data is consistent with the energy dependent analysis.
- The analysis of the new data on the η and η' photoproduction confirms the observed earlier $S_{11}(1895)$ state. There is puzzling behavior of the data near the $\eta'p$ threshold.
- The analysis of the $\gamma n \rightarrow K\Lambda$ and $\gamma n \rightarrow K\Sigma$ reactions confirms states in the mass region around 1900 MeV.
- The analysis of the reactions with two pion production provides an important information for the classification of the observed states and branching to the two meson final states.
- The analysis of the Kp collision data reveals the presence of the unknown Σ -hyperons. There is a hope to observe the baryon multiplets and therefore to confirm the states found in the Nucleon-Delta sector.